Available online at www.sciencedirect.com
SCIENCE DIRECT
International Journal of Mass Spectrometry 248 (2006) 61–85
International Journal of Mass Spectrometry
www.elsevier.com/locate/ijms

A comparison of flavonoid glycosides by electrospray tandem mass spectrometry

Raymond E. March [a,*], Errol G. Lewars [a], Christopher J. Stadey [a], Xiu-Sheng Miao [b,1], Xiaoming Zhao [b], Chris D. Metcalfe [b]

[a] *Department of Chemistry, Trent University, 1600 West Bank Drive, Peterborough, ON, Canada K9J 7B8*
[b] *Water Quality Centre, Trent University, 1600 West Bank Drive, Peterborough, ON, Canada K9J 7B8*

Received 11 February 2005; received in revised form 5 September 2005; accepted 6 September 2005

Abstract

A comparison is presented of product ion mass spectra of protonated and deprotonated molecules of kaempferol-3-O-glucoside, quercitin-3-O-glucoside (isoquercitrin), quercitin-3-O-galactoside (hyperoin), apigenin-7-O-glucoside, luteolin-7-O-glucoside, genistein-7-O-glucoside, naringenin-7-O-glucoside (prunin), luteolin-4′-O-glucoside, luteolin-6-C-glucoside (homoorientin, known also as isoorientin), apigenin-8-C-glucoside (vitexin), and luteolin-8-C-glucoside (orientin) together with the product ion mass spectrum of deprotonated kaempferol-7-O-glucoside. All isomeric ions were distinguishable on the basis of their product ion mass spectra. For protonated 3-O-, 7-O-, and 4′-O-glycosides at a collision energy of 46–47 eV, homolytic cleavage of the O-glycosidic bond yielded aglycon Y^+ ions, whereas in deprotonated 3-O-, 7-O-, and 4′-O-glycosides, heterolytic and homolytic cleavage of the O-glycosidic bond yielded radical aglycon $(Y–H)^{\bullet -}$ and aglycon (Y^-) ions. In each case, fragmentation of either the glycan or the aglycon or both was observed. For 6-C- and 8-C-glycosides at a collision energy of 46–47 eV, fragmentation was restricted almost exclusively to the glycan. For luteolin-6-C-glucoside, the integrity of the aglycon structure is preserved at the expense of the glycan for which some 30 fragmentations were observed. Breakdown curves were determined as a function of collision energy for protonated and deprotonated luteolin-6-C-glucoside. An attempt has been made to rationalize the product ion mass spectra derived from C–O- and C–C-luteolin glucosides in terms of computed structures that indicate significant intramolecular hydrogen bonding and rotation of the B-ring to form a coplanar luteolin structure. It is proposed that protonated and deprotonated luteolin-6-C-glucoside may afford examples of cooperative interactive bonding that plays a major role in directing fragmentation.

Keywords: Tandem mass spectrometry; Electrospray ionization; Accurate mass; Flavonoid glycosides; Ion dissociation

1. Introduction

The study of the ubiquitous class of phytochemicals known as the flavonoids [1] has been confined largely heretofore to their distribution in the plant kingdom, elucidation of their structures, and the pathways by which they are synthesized. Flavonoids are found primarily in petals, the foliage of trees and bushes, and are distributed widely in the edible parts of plants. Plants synthesize flavonoids and secondary metabolites for protection against pathogens and herbivores. The flavonoids were reviewed extensively in 1994 [2]. The predominant form of naturally occurring flavonoids in plants is that of a flavonoid glycoside. All flavonoid glycosides have a C_{15} phenyl-benzopyrone skeleton to which glycosidic moieties are attached via either an O atom (–O–) or a skeletal C atom (–C–). Because of their antioxidant and anticancer properties, flavonoid glycosides present in foodstuffs and nutraceuticals have received much attention recently.

Flavonoids and isoflavonoids may be of ecotoxicological importance because they are present in the heartwood of tree species used for wood pulp [3,4] and are found in a variety of fruits and vegetables. Plants of the Leguminosae family (e.g., soy, lupin) contain isoflavones that are important components of the diets of humans and animals. A review of genistein, including its distribution in plants, estrogenic properties, cancer chemopreventative activity, and chemopreventative activity for cardiovascular disease was published in 2002 [5]. Flavonoids are of environmental significance because several flavonoid aglycons

* Corresponding author. Tel.: +1 705 748 1011 7361; fax: +1 705 748 1625.
E-mail address: rmarch@trentu.ca (R.E. March).
[1] Present address: ArQule, Inc., 19 Presidential Way, Woburn, MA 01801, USA.

1387-3806/$ – see front matter © 2005 Elsevier B.V. All rights reserved.
doi:10.1016/j.ijms.2005.09.011

(flavonoid glycosides that have lost the sugar or glycan moiety) are known to be biologically active [6] while some isoflavones are also phytoestrogens [7,8] that have radical scavenger [9,10] and anticarcinogenic [11,12] activities. The estrogenic activity of flavonoids has been characterized relative to that of estradiol [13,14]. While phytochemicals in the heartwood and sapwood of trees render the wood resistant to disease [3], flavonoids in mammals can affect reproduction by acting upon the pituitary-gonadal axis, either as competitors for steroid receptor sites [15] or by inhibiting aromatase [16]. Flavonoids are present also in herbal medicines [17] and preventative therapeutics [11].

Although structural elucidation of flavonoid glycosides was attempted using electron impact mass spectrometry [18], the advent of fast atom bombardment (FAB), atmospheric pressure chemical ionization (APCI) and, particularly, electrospray ionization (ESI) combined with tandem mass spectrometry (MS/MS) has permitted much more rapid study of the flavonoids, their ion chemistry, and the determination of flavonoids in low concentrations in aqueous systems. Cuyckens and Claeys have reviewed recently the role of mass spectrometry in the structural analysis of flavonoids [19].

FAB/MS/MS has been employed for structure determination of steroid and flavonoid glycosides [20,21], differentiation of 6-C- and 8-C-glycosidic flavonoids [22,23] and of O-diglycosyl, O–C-diglycosyl, and di-C-glycosyl flavonoids [24], and the investigation of prenylated flavonoids using B^2/E^2 and B/E linked scans [25,26]. A review of the application of FAB/MS/MS to the study of flavonoid glycosides has been presented [27]. Nuclear magnetic resonance (NMR) spectroscopy has been combined with FAB/MS/MS [28] and with high-performance liquid chromatography/MS for the structural characterization of flavonoids and flavonoid-O-glycosides [29,30]. In addition, ^{13}C NMR spectra have been obtained for a number of flavonoids [31], and both ^{13}C and ^{1}H NMR spectra have been reported for acylated derivatives of apigenin-7-O-glucoside [32]. Thermospray coupled with liquid chromatography/tandem mass spectrometry, LC/MS/MS, has been used for the characterization of flavonoids [33] and the rapid screening of fermentation broths for flavones [34]. Using ion spray LC/MS/MS, parent ion scans of two protonated aglycons, quercitin and kaempferol, indicated the presence of more than 12 flavonol glycosides among nine hop varieties [35]. Ion spray LC/MS/MS has been used also for the characterization of flavonoids in extracts from *Passiflora incarnata* [36,37]. APCI/MS/MS has been employed for the quantitation of xanthohumol and related prenylflavonoids in hops and beer [38], for a study of flavonone absorption following naringin, hesperidin, and citrus administration [39], and for the identification of 26 aglycons from the leaf surfaces of Chrysothamnus [40]. ESI/MS/MS has been employed for analysis of 6′-O-malonylated β-D-glucosides in plants [41], and for the investigation of gas phase apigenin anionic clusters [42] and of Na^+-bound clusters of quercetin [43].

ESI/MS/MS has been employed also for the investigation of 14 flavonoids [44], flavonoid aglycons [45], characterization of flavonoid-O-diglycosides [46,47], and kaempferol [48] and genistein-7-O-glucoside [49] at high mass resolution. McCullagh et al. [50] have reported ESI/MS/MS mass spectra for $[M–H]^-$ of isoorientin, orientin, and vitexin. Collision-induced homolytic and heterolytic cleavage of the O-glycosidic bond in flavonoid glycosides yielded radical aglycon $(Y–H)^{\bullet -}$ and aglycon (Y^-) product ions, respectively. The relative abundance of the radical aglycon to the aglycon product ion from flavonol-3-O-glycosides varied with the nature and position of the sugar substitution and increased with increasing number of hydroxyl substituents in the B ring and in the order kaempferol < quercetin < myricetin-3-O-glycoside. Radical aglycon production from apigenin-7-O-glucoside exceeded that from luteolin-7-O-glucoside [51,52].

The formation and CID of metal/flavonoid complexes using ESI/MS/MS has been employed for the differentiation of flavonoid isomers. Frequently this approach yields more distinctive fragmentation patterns than those observed for protonated or deprotonated flavonoids [53,54]; in this manner, glycosides of apigenin, quercetin, and luteolin have been differentiated. Zhang and Brodbelt have investigated also the gas-phase hydrogen/deuterium exchange and conformations of deprotonated flavonoids [55] and quantification by LC/MS of the main flavonoids in grapefruit juice, naringin and narirutin; structural differentiation was accomplished by LC/MS/MS [56].

The combination of MS/MS with ESI has proven to be a valuable technique that has great sensitivity, specificity, mass range, and mass resolution. In this work, a study of 12 flavonoid glycosides has been carried out using ESI/MS/MS at high mass accuracy. The flavonoid glycosides were selected as being representative of the variety of flavonoid moiety and the location of glycoside attachment in flavonoid glycosides found naturally. Eleven flavonoid glucosides were investigated together with a single flavonoid galactoside. Although glucose is the most common sugar in flavonoid glycosides, galactose along with rhamnose, xylose, and arabinose are not uncommon [57,58].

Product ion mass spectra as a function of collision energy of $[M + H]^+$ and $[M–H]^-$ ion species of each flavonoid glycoside, M, were obtained at high mass accuracy with a quadrupole/time-of-flight instrument. Product ions were identified within an average mass accuracy of ±1.5 mDa. The application of enhanced cone voltages permitted MS/MS/MS operation. The results obtained permit construction of a fragmentation map or scheme for each flavonoid glycoside; selected fragmentation schemes are shown here. Chemical computations of ion and neutral structures were carried out using both a semiempirical and an ab initio method.

2. Objectives

The objectives of this research work were to acquire product ion mass spectra for protonated and deprotonated flavonoid glycosides in support of LC/MS/MS analysis, to identify the position of attachment of the glycoside, for example, to distinguish between 3-O-, 7-O-, and 4′-O-glycosidic flavonoids and to differentiate between O- and C-glycosides, to examine glycan cross-ring cleavage, to determine the energy dependence of the glycan cross-ring cleavage in C-bonded glycosides, and to

Table 1
Flavonoid glycosides examined, solution concentration used, molecular weight, and product ion mass spectra displayed

Type	3-O-Glu	3-O-Gal	7-O-Glu	4′-O-Glu	6-C-Glu	8-C-Glu
Flavone 5,7,4′-tri-hydroxy	–	–	Apigenin[b], 188 ppm, MW 432	–	–	Apigenin[a,b] (vitexin) 196 ppm), MW 432
Flavone 3,5,7,4′-tetra-hydroxy	Kaempferol, 80 ppm, MW 448	–	Kaempferol[b], 120 ppm, MW 448	–	–	–
Flavone 5,7,3′,4′-tetra-hydroxy	–	–	Luteolin[a,b], 94 ppm, MW 448	Luteolin[a], 170 ppm, MW 448	Luteolin[a,b] (homoorientin), 80 ppm, MW 448	Luteolin[a,b] (orientin), 80 ppm MW 448
Flavone 3,5,7, 3′,4′-penta-hydroxy	Quercitin (isoquercitrin), 244 ppm, MW 464	Quercitin[a,b], 110 ppm, MW 464	–	–	–	–
Isoflavone 5,7,4′-tri-hydroxy	–	–	Genistein[b], 150 ppm, MW 432	–	–	–
Flavanone 5,7,4′-tri-hydroxy	–	–	Naringenin (prunin), 116 ppm, MW 434	–	–	–

[a] Product ion mass spectrum of $[M+H]^+$ is given.
[b] Product ion mass spectrum of $[M-H]^-$ is given.

attempt to correlate product ion mass spectra with computed ion structures.

3. Experimental

ESI-MS and MS/MS experiments were performed on a triple stage mass spectrometer (Quattro LC, Micromass, Manchester, UK) and a Q-TOF 2™ mass spectrometer (Micromass, Manchester, UK) each with a Z-spray™ ES source. The ES source potential on the capillary was 3.0 kV. The sampling cone voltage was varied from 20 to 140 V for ES mass spectra. The quadrupole mass filter to the TOF analyzer was set with LM and HM resolution of 15.0 (arbitrary units), which is equivalent to a 1.0 Da mass window for transmission of precursor ions. The source block and desolvation temperatures were set at 80 and 150 °C, respectively. CID of mass-selected ions was performed in an rf-only quadrupole collision cell. UHP argon was used as the collision gas at 10 psi inlet pressure for CID experiments. Signal detection was performed with a reflector, microchannel plate (MCP) detector and time-to-digital converter. Mass calibration was carried out using a NaI/CsI standard solution from *m*/*z* 50–1000. Data acquisition and processing were carried out using software MassLynx NT version 3.5 supplied with the instrument. The MS survey range was *m*/*z* 50–1000 and the duration of each scan was 1.0 s with an interscan delay of 0.1 s. Mass spectra were accumulated over a period of 60 s or more for both single analyzer profiles and CID experiments. For each of the ion species examined, the lock mass in each product ion mass spectrum was the calculated monoisotopic mass/charge ratio of the precursor ion. The concentration of each compound examined is shown in Table 1. Product ions were identified within a mass accuracy of ±1.5 mDa using the QTOF II.

Kaempferol-7-O-glucoside was isolated at the University of Medical Science, Poznan, Poland; apigenin-7-O-glucoside, luteolin-7-O-glucoside, genistein-7-O-glucoside, and apigenin-8-C-glucoside (vitexin), kaempferol-3-O-glucoside, quercitin-3-O-glucoside (isoquercitrin), naringenin-7-O-glucoside (prunin), quercitin-3-O-galactoside (hyperoin) were obtained from the Roth Co., Germany; luteolin-4′-O-glucoside and luteolin-8-C-glucoside (orientin), luteolin-6-C-glucoside (homoorientin, known also as isoorientin) were obtained from the Indofine Co., USA.

The analyte solutions were prepared using methanol and water (1:1) at a concentration of 80–200 μg mL^{-1}. The solutions were infused to the ES source using a Harvard Apparatus Model 11 syringe pump (Harvard Apparatus, Holliston, MA) at a flow rate of 10 μL min^{-1}. For the investigation of appearance energies of product ions resulting from cross-ring cleavages, solutions of 1 ppm were used in conjunction with the Quattro LC instrument.

For the calculation of molecular geometries and frequencies, both semiempirical PM3 [59], and ab initio or density functional theory (DFT) [59] methods were used. The semiempirical method was applied to some 15 structures because the speed of semiempirical methods makes practical such calculations on a series of fairly large molecules; the DFT method was applied to a subset of six structures. The PM3 method, imple-

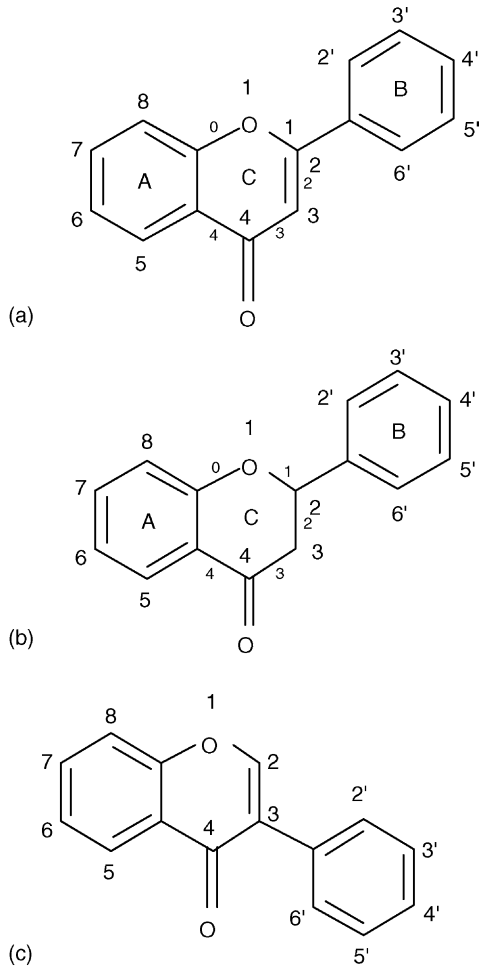

Scheme 1. Structures and numbering schemes: (a) flavones; (b) flavanones; and (c) isoflavones.

mented in SPARTAN [60], was used rather than the other popular semiempirical method, AM1 [61], because PM3 appears to treat hydrogen bonding somewhat better than does AM1 [62]; like AM1, PM3 gives good geometries for conventional molecules [59]. The computed structures were characterized as relative minima on the PM3 potential energy surface by the absence of imaginary frequencies in their calculated IR spectra [63]; they should be regarded as plausible geometries, and not necessarily as global minima, in view of the many degrees of rotational freedom available to these molecules.

4. Results and discussion

The product ion mass spectra for the flavonoid glycosides examined here are discussed in order of their appearance in Table 1. The numbering schemes for flavones, flavanones and isoflavones, are shown in Scheme 1; the small numerical font in Scheme 1 identifies the bonds in the C ring. A systematic ion nomenclature for flavonoid aglycons has been proposed [64] that is conceptually similar to that introduced for the description of carbohydrate fragmentations in product ion mass spectra of glycoconjugates [65]. The nomenclature and diagnostic fragmentations of $[M–H]^-$ of genistein-7-O-glucoside are shown in

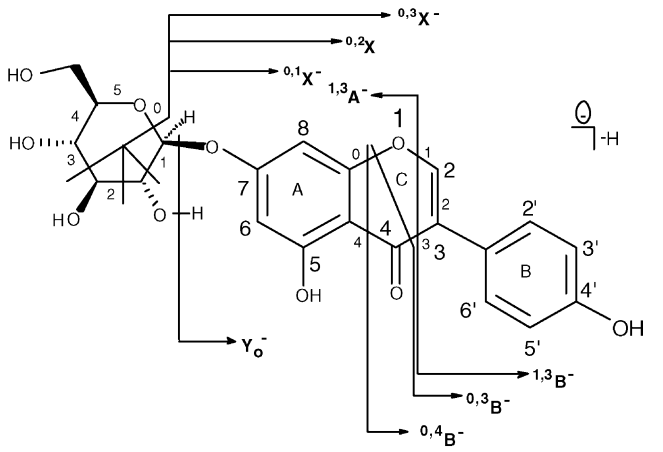

Scheme 2. Nomenclature and diagnostic fragmentations of $[M–H]^-$ of genistein-7-O-glucoside.

Scheme 2. For free aglycons, the $^{i,j}A^+$ (or $^{i,j}A^-$) and the $^{i,j}B^+$ labels designate primary product ions containing intact A and B rings, respectively, in which the superscripts indicate the C-ring bonds that have been broken. In Scheme 2, the C-ring bonds and the glucose ring bonds are numbered with a small font, the carbon atoms in the A, B, and C rings are labeled with a larger font, and the primary fragmentations are indicated. Ions resulting from cross-ring cleavages in the sugar residue are denoted with X labels.

4.1. Product ion mass spectra of three 3-O-glycosides

Product ion mass spectra of the protonated and deprotonated 3-O-glucosides of kaempferol and quercitin were compared so

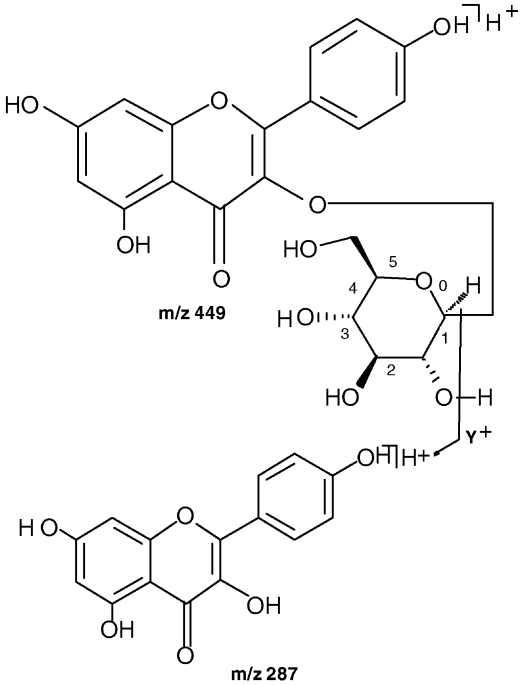

Scheme 3. Fragmentation scheme of $[M+H]^+$ of kaempferol-3-O-glucoside, *m/z* 449.

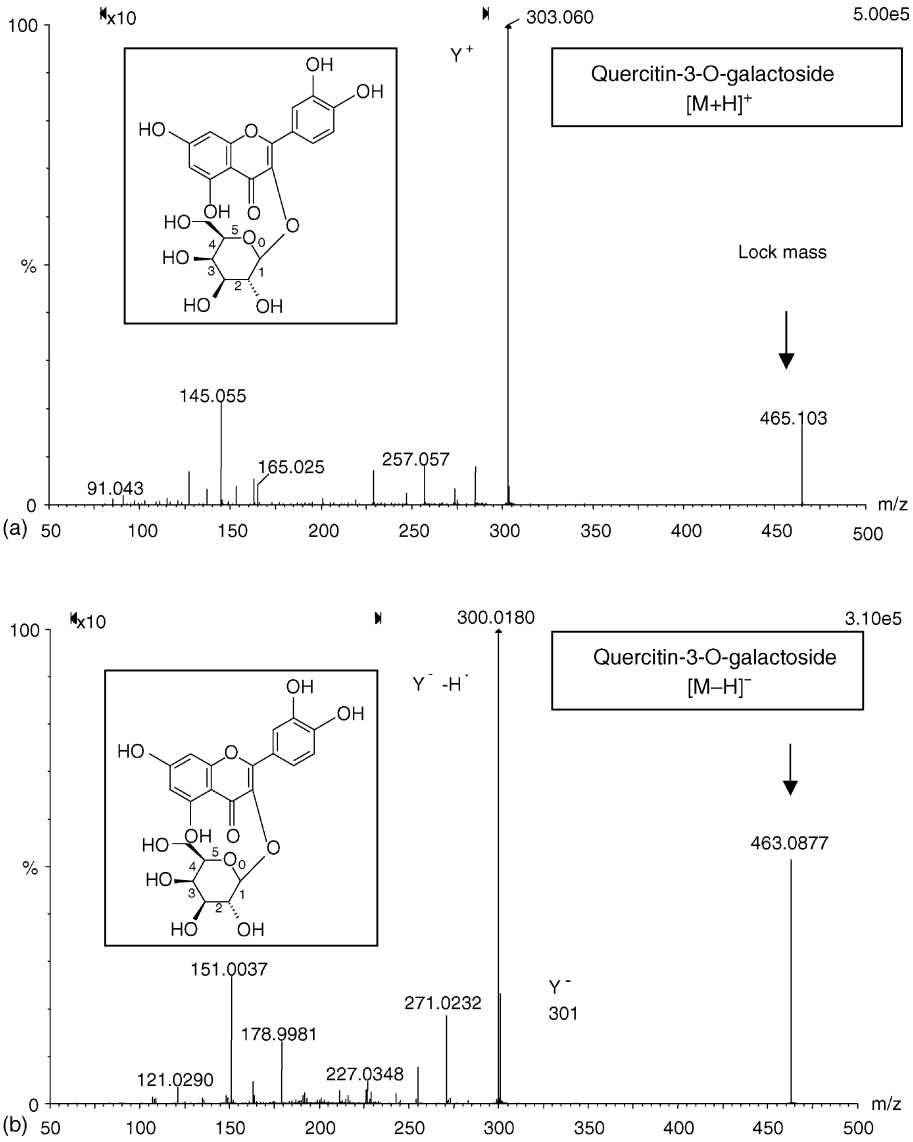

Fig. 1. Product ion mass spectra of quercitin 3-O-galactoside obtained at a collision energy of 47 eV and cone voltage of 45 V: (a) $[M+H]^+$ (*m/z* 465.1030); (b) $[M–H]^-$ (*m/z* 463.0877).

as to determine what influence, if any, is exerted by the presence of the 3′-hydroxy substituent in quercitin-3-O-glucoside. The inclusion of quercitin-3-O-galactoside in this study afforded an opportunity for comparison of the fragmentation of two different glycosides of a common flavone, quercitin.

4.1.1. Protonated kaempferol-3-O-glucoside, quercitin-3-O-glucoside, and quercitin-3-O-galactoside

The protonated molecules $[M+H]^+$ of kaempferol-3-O-glucoside, quercitin-3-O-glucoside and quercitin-3-O-galactoside upon dissociation at a collision energy of 46–47 eV yield the Y^+ ion in each case from the loss of 162 Da as shown in Scheme 3 for protonated kaempferol-3-O-glucoside. Similarly, the Y^+ ion is the base peak in FAB mass spectra of the compounds [21]; however, unlike the FAB mass spectra, the $[M+H–O]^+$ and Z^+ ions were not detected in the product ion mass spectra. For protonated kaempferol- and quercitin-3-O-glucosides, neither fragmentation of the glucose moiety nor product ions of $m/z > 150$ from the flavone moiety were observed. Other than the Y^+ ion for each compound, *m/z* 287 and *m/z* 303 for the 3-O-glucosides of kaempferol and quercitin, respectively, there is little information concerning the identity of the precursor ion.

For protonated quercitin-3-O-galactoside, extensive fragmentation of the aglycon was observed as shown in Fig. 1(a) and illustrated in Scheme 4. Cross-ring cleavages of the C-ring lead to the observation of the $^{1,3}A^+$ (*m/z* 153) and $^{1,4}A^+ + 2H^\bullet$ (*m/z* 127) product ions. Nine product ion species, formed by rearrangement processes with the expulsion of one or more of H_2O, CO, $HCO^\bullet$, and CH_2O, were observed. The *m/z* 145 product ion is of particular interest here; the elemental composition was determined by accurate mass measurement as $C_6H_9O_4^+$ with a mass error of −4 mDa. The relatively high H:C ratio in $C_6H_9O_4^+$ indicates that *m/z* 145 does not arise from the Y^+ ion but, rather, from the galactose glycan as the $B^+–H_2O$ ion. Because extensive glycan fragmentation is observed for several

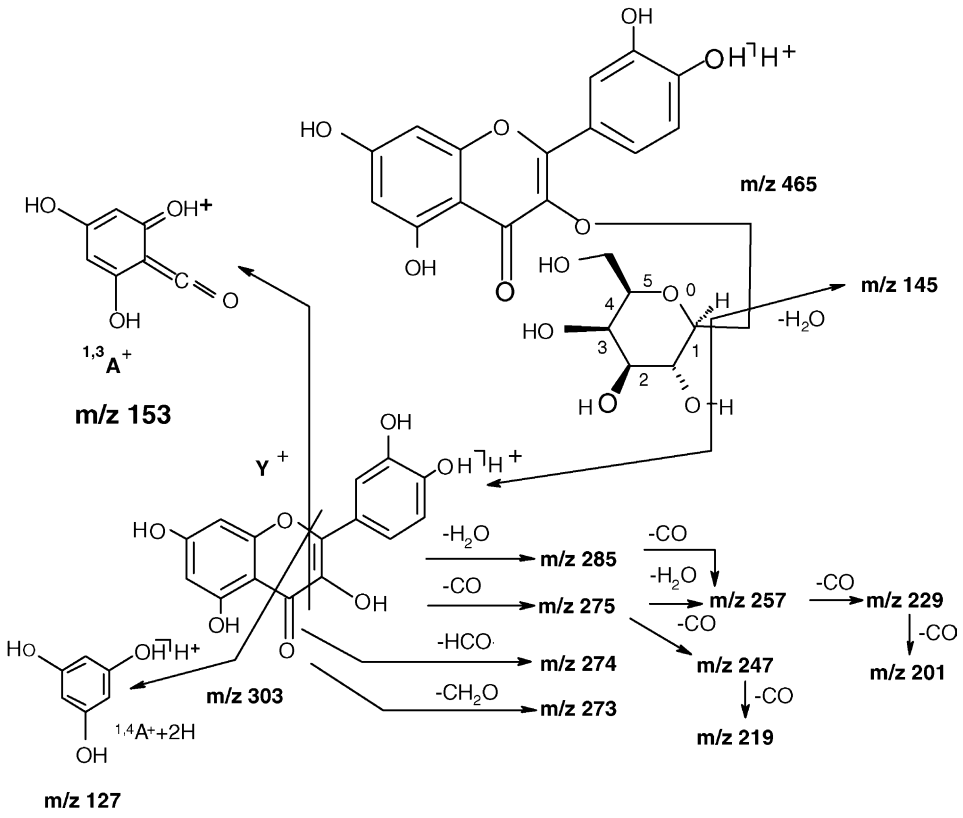

Scheme 4. Fragmentation scheme of $[M + H]^+$ of quercitin-3-O-galactoside, *m*/*z* 465.

flavonoid glycosides, as is discussed below, a study of protonated and deprotonated sugar molecules (pentoses, hexoses, and disaccharides) has been carried out in this laboratory [66]. In this study [66], a product ion of *m*/*z* 145 was observed as a major component of the product ion mass spectrum of each of the disaccharides sucrose, maltose, α-lactose, and β-lactose; the elemental composition was determined as $C_6H_9O_4^+$ with a mass accuracy of 1.4 ± 0.8 mDa. In a recent study of kaempferol diglycosides [54], the loss of 146 Da was indicative of the initial elimination of the outer sugar unit as a deoxy-hexose sugar. In the case of protonated quercitin-3-O-galactoside, the loss of the sole sugar unit as a charged deoxy-hexose sugar of *m*/*z* 145 may be used for distinguishing galactosides from glucosides. Other flavonoid galactosides should be examined to determine whether formation of the B^+–H_2O ion is common to all such compounds; however, flavonoid galactosides are not available readily.

4.1.2. Deprotonated kaempferol-3-O-glucoside, quercitin-3-O-glucoside and quercitin-3-O-galactoside

Collision-induced dissociation (not shown) of $[M–H]^-$ of kaempferol-3-O-glucoside lead to observation of the Y^- ion (*m*/*z* 285) together with formation of the radical anion $(Y–H)^{\bullet -}$ (*m*/*z* 284) as shown in Scheme 5. The variation of the ratio of ion signal intensities of the Y^- and $(Y–H)^{\bullet -}$ ions is discussed in greater detail in Section 2.ii.a. As the collision energy is increased so is the degree of fragmentation of the Y^- ion to form *m*/*z* 255 by loss of CH_2O and *m*/*z* 227 by the further loss of CO. Fragmentation of the glucose moiety was observed only for $[M–H]^-$ of kaempferol-3-O-glucoside; the observed loss of 120 Da to form the $^{0,2}X^-$ ion is due to 0,2 scission of the glycoside as is shown in Scheme 5.

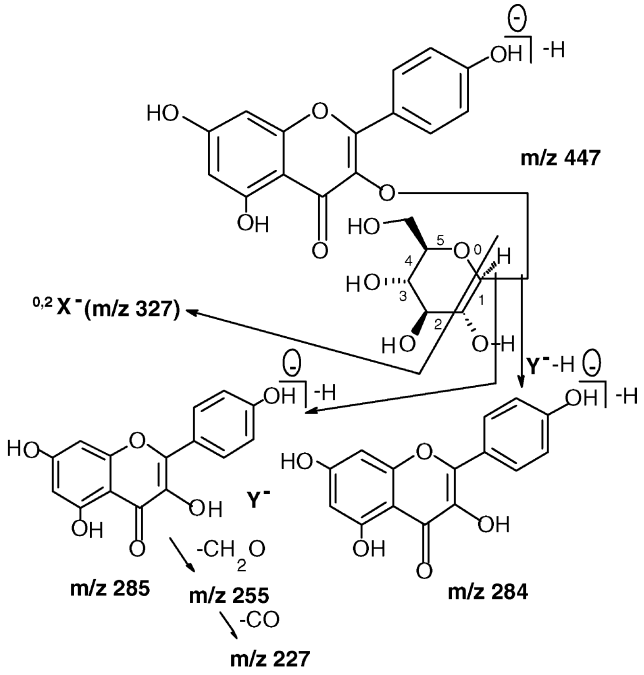

Scheme 5. Fragmentation scheme of $[M–H]^-$ of kaempferol-3-O-glucoside, *m*/*z* 447.

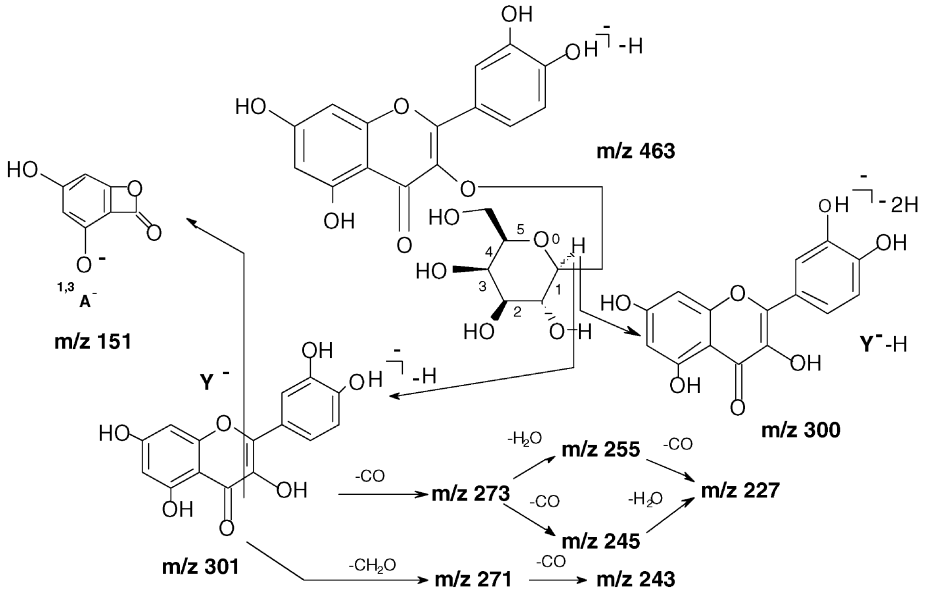

Scheme 6. Fragmentation scheme of $[M–H]^-$ of quercitin-3-O-galactoside, *m/z* 463.

The product ion mass spectra of $[M–H]^-$ of quercitin-3-O-glucoside (not shown) and quercitin-3-O-galactoside (Fig. 1(b)) show also the Y^- ion (*m/z* 301) and the radical anion $(Y–H)^{\bullet-}$ (*m/z* 300). Additional product ions arose from fragmentation of the aglycon alone, that is, fragmentation of the Y^- ion only. The fragmentation scheme for $[M–H]^-$ of quercitin-3-O-galactoside is given in Scheme 6. Only the product ions *m/z* 271 due to the loss of CH_2O and *m/z* 255 due to the combined losses of H_2O and CO were common to both quercitin-3-O-glucoside and quercitin-3-O-galactoside. No product ions arising from the $(Y–H)^{\bullet-}$ species were observed in the product ion mass spectra of these deprotonated glycosides. Negative ion FAB mass spectra [21] of these compounds showed the Y^- ion as the base peak in each case; the $[M–H–O]^-$ and Z^- ions observed in FAB mass spectra were not detected in the product ion mass spectra. Therefore, the 3-O-glucoside of quercitin can be distinguished from its 3-O-galactoside on the basis of the product ion mass spectra of $[M–H]^-$.

4.2. Product ion mass spectra of four 7-O-glucosides

Product ion mass spectra of protonated and deprotonated 7-O-glucosides of apigenin, genistein (isomeric with apigenin), and naringenin were observed so as to compare the behavior of a tri-hydroxy flavone with those of a tri-hydroxy isoflavone and a tri-hydroxy flavanone. The inclusion of luteolin-7-O-glucoside permitted a comparison of a tetra-hydroxy flavone with that of a tri-hydroxy flavone, apigenin-7-O-glucoside. In addition, the

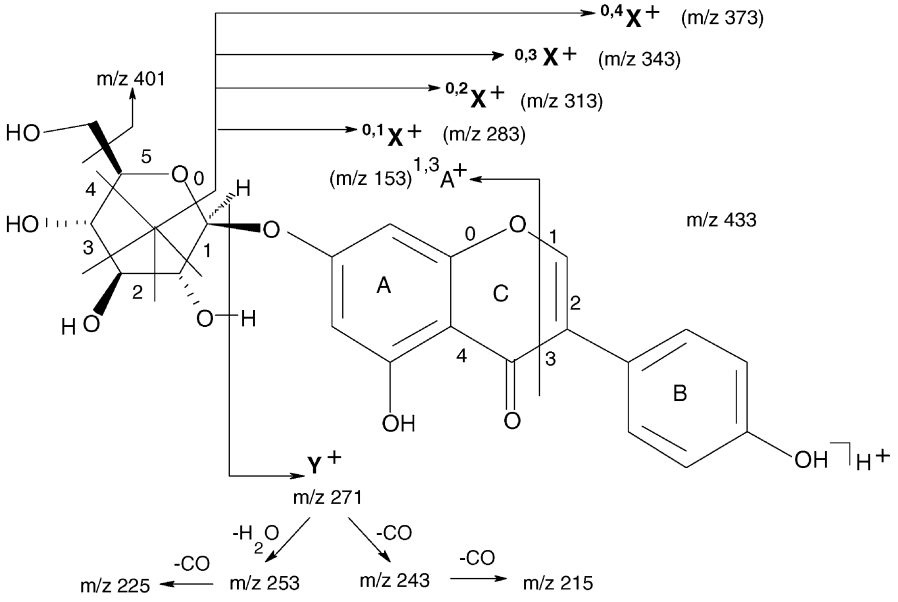

Scheme 7. Fragmentation scheme of $[M + H]^+$ of genistein-7-O-glucoside, *m/z* 433.

Table 2
Neutral losses observed (√) in glucose fragmentation of $[M+H]^+$ ions of apigenin-7-O-glucoside, luteolin-7-O-glucoside, genistein-7-O-glucoside, and naringenin-7-O-glucoside

	1–2 H_2O	32 Da	46 Da	60 Da	$^{0,4}X^+$ [a]	78 Da $^{0,4}X^+$–w [b]	90 Da $^{0,3}X^+$ [c]	92 Da $^{0,3}X^+$–2H• [d]	120 Da $^{0,2}X^+$	122 Da $^{0,2}X^+$–2H•	132 Da $^{1,5}X^+$–2H•	148 Da $^{0,1}X^+$–2H•	150 Da $^{0,1}X^+$	152 Da $^{0,1}X^+$–2H•	162 Da Y^+
Apigenin	–	–	–	–	–	–	–	–	–	–	–	–	–	–	√
Luteolin	–	–	–	–	√	–	–	–	–	–	–	√	–	–	√
Genistein	√	√	√	√	–	√	√	√	√	√	√	–	√	√	√
Naringenin	–	–	–	–	–	–	–	–	–	–	–	–	–	–	√

[a] $^{0,4}X^+$ or $^{1,3}X^+$ or $^{2,4}X^+$.
[b] $^{0,4}X^+$–w or $^{1,3}X^+$–w or $^{2,4}X^+$–w.
[c] $^{0,3}X^+$ or $^{1,4}X^+$.
[d] $^{0,3}X^+$–2H• or $^{1,4}X^+$–2H•.

product ion mass spectrum of kaempferol-7-O-glucoside, isomeric with luteolin-7-O-glucoside, was examined.

4.2.1. Protonated 7-O-glucosides of apigenin, luteolin, genistein, and naringenin

The product ion mass spectra (not shown) of the $[M+H]^+$ ions of protonated 7-O-glucosides of apigenin, luteolin, genistein, and naringenin showed principally the Y^+ product ion due to the loss of 162 Da, as did the FAB mass spectra for the 7-O-glucosides of apigenin [21] and luteolin [21,64]. Only genistein-7-O-glucoside showed extensive fragmentation of both the aglycon and glucose moieties and the principal fragmentations are shown in Scheme 7 [49] and in Table 2. The ions of *m/z* 415 and 397 are associated with the losses of one and two water molecules, respectively. *m/z* 401 can be formed by the loss of the primary alcohol group as methanol and *m/z* 387 by 4,5 scission with the loss of the elements of ethanol. Further fragmentations of the glucose moiety gave rise to the $^{0,4}X^+$, $^{0,3}X^+$, $^{0,3}X^+$–2H•, $^{0,2}X^+$, $^{0,2}X^+$–2H•, $^{1,5}X^+ + 2H^•$, $^{0,1}X^+$, and $^{0,1}X^+$–2H• ions at *m/z* 373, 343, 341, 313, 311, 301, 283, and 281, respectively. Fragmentation of the glucose moiety in luteolin-7-O-glucoside yielded only the $^{1,3}X^+$–*w* (where *w* represents an H_2O molecule) and $^{0,1}X^+ + 2H^•$ ions of *m/z* 371 and 301, respectively. It is remarkable that the fragmentations of the glucose moiety in genistein-7-O-glucoside and luteolin-7-O-glucoside are entirely complementary. As shown in Table 2, no fragmentations of the glycan were observed for the 7-O-glucosides of apigenin and naringenin.

4.2.2. Deprotonated 7-O-glucosides of apigenin, kaempferol, luteolin, genistein, and naringenin

The flavone apigenin is isomeric with the isoflavone genistein and each is hydroxylated in the 4′-position on the B ring. The flavones kaempferol and luteolin are isomeric. Tri-hydroxy naringenin and apigenin are hydroxylated in the same positions. These compounds are compared with respect to primary fragmentation of $[M–H]^–$, aglycon fragmentation, and glucose fragmentation.

4.2.2.1. Primary fragmentation of [M–H]$^–$. The principal features of the product ion mass spectra of $[M–H]^–$ ions of the 7-O-glucosides are the formation of the $Y^–$ and $(Y–H)^{•–}$ ions as shown in Scheme 8 for apigenin-7-O-glucoside. The $Y^–$ ion is formed by re-arrangement with the loss of 162 Da and the $(Y–H)^{•–}$ radical anion is formed by scission with the loss of 163 Da [49,51]. In Fig. 2(a) and (b) for apigenin-7-O-glucoside and genistein-7-O-glucoside, respectively, the $Y^–$ ion is observed at *m/z* 269; in Fig. 2(c) and (d) for kaempferol-7-O-glucoside and luteolin-7-O-glucoside, respectively, the $Y^–$ ion is observed at *m/z* 285. For the 7-O-glucosides of apigenin and genistein, the scission reactions are dominant at a collision energy of 46–47 eV whereas, for the 7-O-glucosides of kaempferol and luteolin, the converse holds. The propensity for radical anion formation from apigenin-7-O-glucoside exceeds that from luteolin-7-O-glucoside [51,52]. For genistein-7-O-glucoside, the variation of the ratio of the ion signal intensities of *m/z* 268 $(Y–H)^{•–}$ and *m/z* 269 $(Y^–)$ ions as a function of

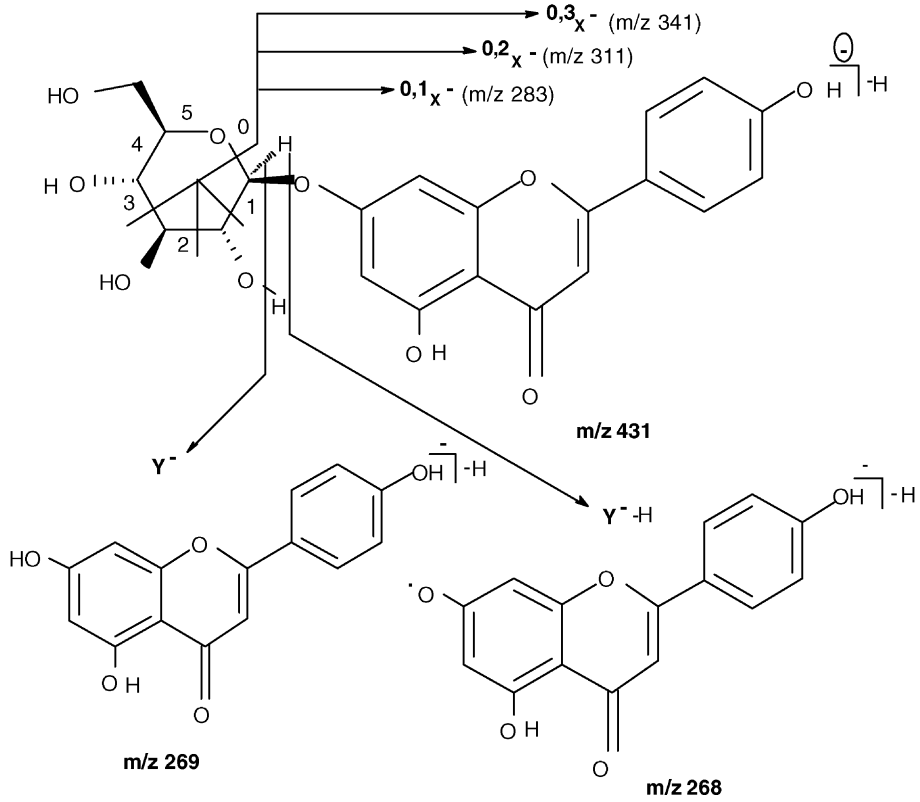

Scheme 8. Fragmentation scheme of $[M–H]^-$ of apigenin-7-O-glucoside *m/z* 431.

collision energy is shown in Fig. 2 of reference [49]. At low collision energies (~15–30 eV), the rearrangement reaction product dominates however, as collision energy is increased, the scission product increases relative to that of the rearrangement product. While the product ion mass spectra obtained at high mass accuracy of the $(Y–H)^{\bullet -}$ and Y^- ions are discussed elsewhere [49], the principal features are: (i) hydrogen atom loss from *m/z* 268 to form *m/z* 267 and the combined losses of $CHO^\bullet$ and CO to form *m/z* 211, and (ii) the major product ion from *m/z* 269 is the $^{0,3}B^-$ ion of *m/z* 133.

The $[M–H]^-$ ion of naringenin-7-O-glucoside fragments to the Y^- ion (*m/z* 271); the Y^- ion forms the base peak in positive ion FAB mass spectra of the 7-O-glucosides of apigenin and luteolin [21]. The $(Y–H)^{\bullet -}$ ion was conspicuous by its absence.

4.2.2.2. Aglycon fragmentation. Other than the $(Y–H)^{\bullet -}$ radical anion, no aglycon fragmentation was observed in the product ion mass spectra of the $[M–H]^-$ ions of apigenin-7-O-glucoside and genistein-7-O-glucoside at a collision energy of 20 eV. In Fig. 2(a), the ion signals in the mass range $60 < m/z < 260$ have been magnified ×15 but no discernible ion signals were observed. Ion signals were observed showing fragmentation of the glucose moiety and these are discussed below.

The product ion mass spectrum of kaempferol-7-O-glucoside shown in Fig. 2(c) differs markedly from those of apigenin-7-O-glucoside and genistein-7-O-glucoside in that there is appreciable fragmentation of the aglycon. Ten product ion species from the aglycon were observed of which the major fragments were of *m/z* 257, 241 and 151. The ion signal intensity of *m/z* 151 was some 26% of the base peak in Fig. 2(c). It is proposed that *m/z* 257 and *m/z* 241 are due to the loss of CO and CO_2, respectively, from the Y^- ion in that the elemental compositions of these ion species from accurate mass determination are $C_{14}H_9O_5^-$ and $C_{14}H_9O_4^-$, respectively. The product ion of *m/z* 151 ($^{1,3}A^-$) is an A-ring product ion resulting from a retro-Diels-Alder fragmentation in the C-ring involving1,3 scission. The complementary ion, *m/z* 133, was not observed.

The product ion mass spectrum of luteolin-7-O-glucoside shown in Fig. 2(d) exhibits widespread fragmentation of the aglycon in that some 13 product ion species were observed though of relatively low ion signal intensity; the mass range $60 < m/z < 260$ in Fig. 2(d) has been magnified ×15. The $^{1,3}A^-$ product ion (*m/z* 151) was observed together with the complementary $^{1,3}B^-$ ion (*m/z* 133). *m/z* 256 and 255 are due to loss of CO and CH_2O from *m/z* 284 and 285, respectively. The further losses of CO and CO_2 from *m/z* 255 yield the product ions of *m/z* 227 and 211, respectively. For naringenin-7-O-glucoside, the $^{1,3}A^-$ ion (*m/z* 151) was the sole aglycon product ion arising from further fragmentation of the Y^- ion (*m/z* 271).

4.2.2.3. Fragmentation of the glycan in [M–H]$^-$. Fragmentation of the glycan moiety in the five 7-O-glucosides varied markedly from one $[M–H]^-$ ion to another, as shown in Table 3. The most intense product ions were observed from $[M–H]^-$ of apigenin-7-O-glucoside (Fig. 2(a)) while no discernible product ions other than $(Y–H)^{\bullet -}$ and Y^- ions were observed from $[M–H]^-$ of luteolin-7-O-glucoside (Fig. 2(d)). The product ion mass spectrum of $[M–H]^-$ of apigenin-7-O-glucoside showed

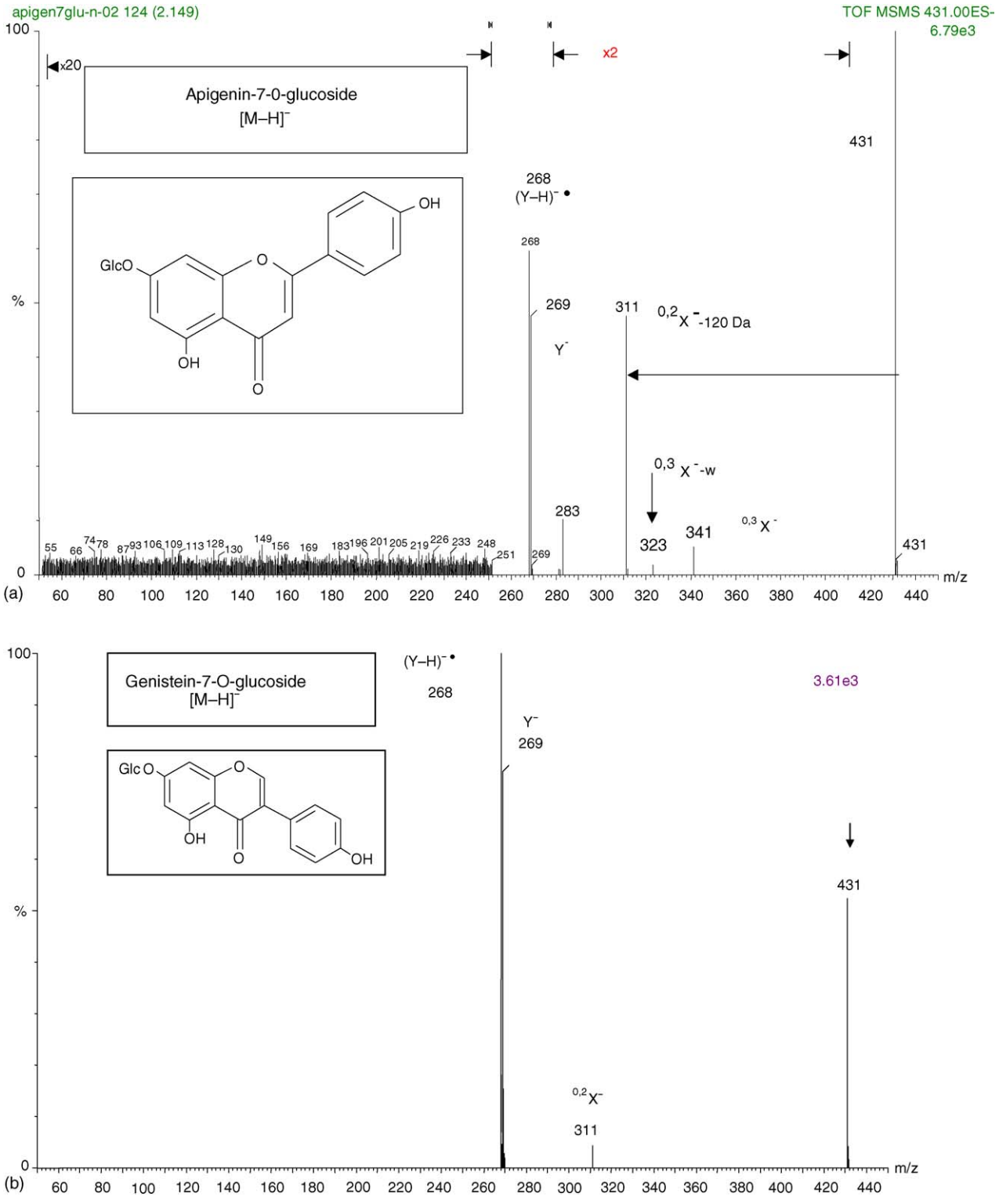

Fig. 2. Product ion mass spectra obtained at a collision energy of 47 eV of $[M–H]^-$ (m/z 431.0978) from (a) apigenin-7-O-glucoside; (b) genistein-7-O-glucoside; (c) kaempferol-7-O-glucoside, and (d) luteolin-7-O-glucoside.

three major fragmentations of the glycan that yield $^{0,3}X^-$ (m/z 341), $^{0,2}X^-$ (m/z 311), and $^{0,1}X^-$ (m/z 283) product ions as shown in Scheme 8. In addition, the product ion of m/z 323 was identified as the $^{0,3}X^-$–w ion where w represents a water molecule. In the product ion mass spectrum of $[M–H]^-$ of genistein-7-O-glucoside, the sole product ion observed is the $^{0,2}X^-$ (m/z 311) ion. Formation of the $^{0,2}X^-$ ion resulting from the loss of 120 Da is common to almost all of the 7-O-glucosides examined here; the sole exception is luteolin-7-O-glucoside. Hydroxylation at the 3′-position (as in luteolin-7-O-glucoside)

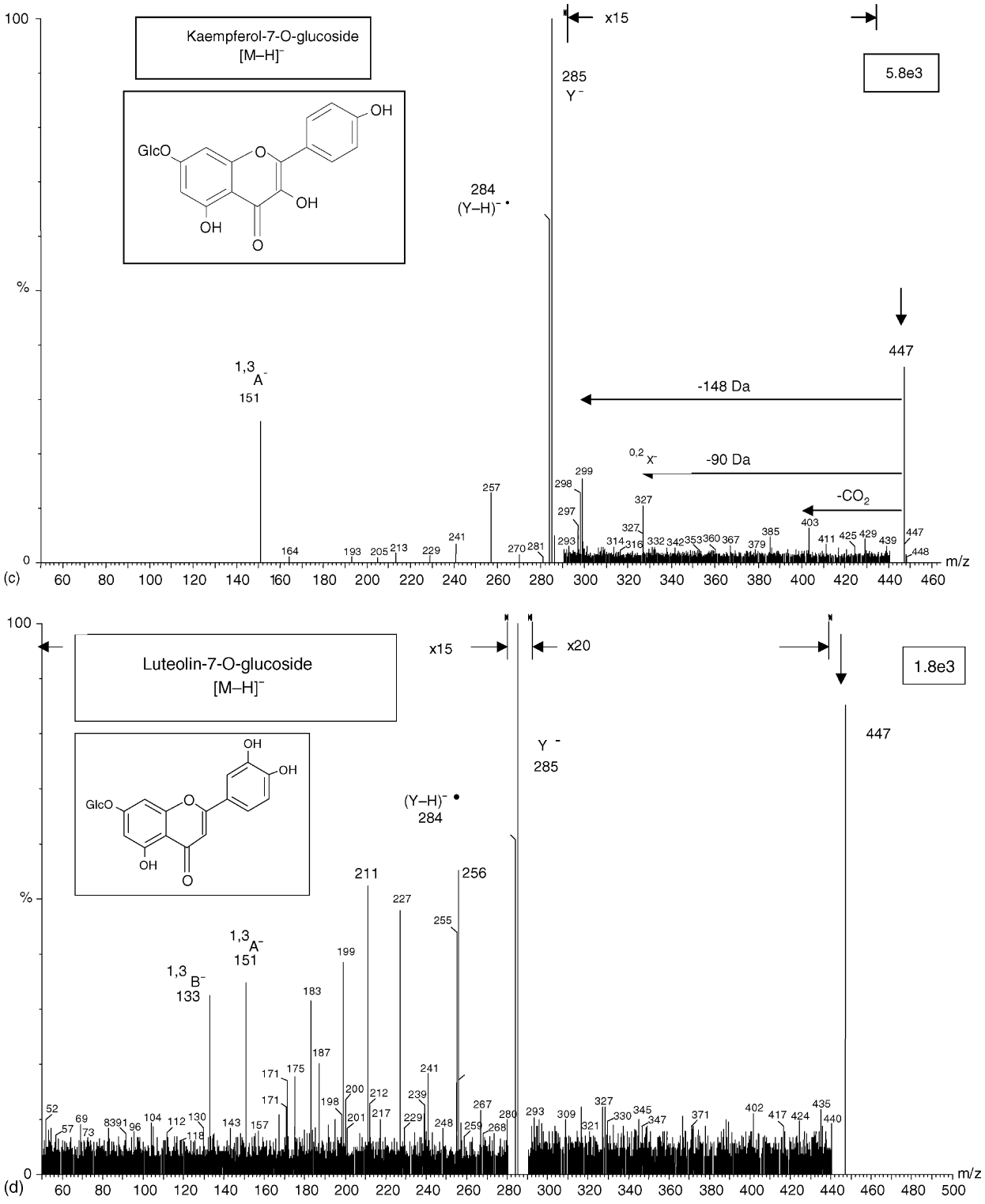

Fig. 2. (*Continued*).

appears to inhibit the 0,2-cleavage of the glucose moiety in both deprotonated (Table 3) and protonated (Table 2) luteolin-7-O-glucoside.

Fragmentation of the glycan in the product ion mass spectrum of kaempferol-7-O-glucoside is different again. The $^{0,2}X^-$ (*m*/*z* 327) ion is observed together with a trio of product ions corresponding to $^{0,1}X^-$ (*m*/*z* 299), $^{0,1}X^-$–H• (*m*/*z* 298), and $^{0,1}X^-$–2H• (*m*/*z* 297) ions. The product ion of *m*/*z* 403 appears to be due to 4,5 scission with the loss of C_2H_4O on the basis of elemental composition from accurate mass measurement. Ions of *m*/*z* 429 and 411 are of very low ion signal intensity; they are identified as due to the loss of one

Table 3
Neutral losses observed (√) in glucose fragmentation of $[M–H]^-$ ions of five 7-O-glucosides

	1–2 H_2O	44 Da	90 Da $^{0,3}X^-$ [a]	108 Da $^{0,3}X^- – w$	120 Da $^{0,2}X^-$	138 Da $^{0,2}X^- – w$	148 Da $^{0,1}X^- + 2H^\bullet$	149 Da $^{0,1}X^- + H^\bullet$	162 Da Y^-	163 Da $Y^- – H^\bullet$
Apigenin	–	–	√	√	√	–	√	–	√	√
Genistein	–	–	–	–	√	–	–	–	√	√
Kaempferol	√ (vw)[b]	√	–	–	√	–	√	√	√	√
Luteolin	–	–	–	–	–	–	–	–	√	√
Naringenin	–	–	–	–	√	√	–	–	–	–

[a] $^{0,3}X^-$ or $^{1,4}X^-$.
[b] vw signifies very low ion signal intensity.

and two water molecules, respectively. In contrast, the product ion mass spectrum of luteolin-7-O-glucoside shows no glycan fragmentation at all. Naringenin shows only the formation of the $^{0,2}X^-$ and $^{0,2}X^- – w$ ions at *m/z* 313 and 295, respectively.

The sole common feature of the product ion mass spectra of deprotonated 7-O-glucosides of apigenin, genistein, kaempferol, and luteolin is loss of the glucose moiety by both rearrangement and scission to form the Y^- and $(Y–H)^{\bullet -}$ ions, respectively. For genistein-7-O-glucoside, there is but a sole additional product ion, the $^{0,3}X^-$ ion. For apigenin-7-O-glucoside, there is no fragmentation of the aglycon and several fragmentations of the glucose moiety whereas for luteolin-7-O-glucoside the converse holds. For kaempferol-7-O-glucoside, there is extensive fragmentation of both the glucose and aglycon moieties.

4.3. Comparison of luteolin-7-O-glucoside and luteolin-4′-O-glucoside

The product ion mass spectra of these compounds are compared with respect to fragmentation of each of $[M–H]^-$ and $[M + H]^+$. In both the positive and negative ion FAB mass spectra [21], luteolin-7-O-glucoside and luteolin-4′-O-glucoside are distinguished only by the ion signal intensity ratio of the $[M + H–O]^+$ and Z^+ ions, and the $[M–H–O]^-$ and Z^- ions, respectively.

4.3.1. Fragmentation of $[M–H]^-$

As discussed above, $[M–H]^-$ ions of luteolin-7-O-glucoside fragment principally to give $(Y–H)^{\bullet -}$ (*m/z* 284) and Y^- (*m/z* 285) ions with the losses of 163 and 162 Da, respectively. $[M–H]^-$ ions of luteolin-4′-O-glucoside fragment principally to give Y^- ions only (*m/z* 285). The product ion mass spectra (not shown) of Y^- (*m/z* 285) from each of these two compounds were obtained consecutively under identical experimental conditions. In each case, the *m/z* 285 species was formed with a cone voltage of 35 V and was isolated in an MS/MS/MS experiment. While the product ion mass spectra are very similar and the base peak in each case is the $^{1,3}B^-$ ion of *m/z* 133, they differ with respect to the formation of *m/z* 284 by H atom loss for luteolin-7-O-glucoside only.

4.3.2. Glucose fragmentation

For the $[M–H]^-$ ions of these compounds, fragmentation of the entire glucose moiety yielded Y^- in each case. Only luteolin-4′-O-glucoside exhibited cross-cleavage to form $^{0,2}X^-$.

4.3.3. Fragmentation of $[M + H]^+$

The product ion mass spectra of $[M + H]^+$ of luteolin-4′-O-glucoside (Fig. 3(a)) and of luteolin-7-O-glucoside (Fig. 3(b)) are similar with respect only to the common base peak (Y^+) of *m/z* 287. The 4′-isomer shows no glucose fragmentation but there is extensive fragmentation of the aglycon; the ion signal intensity of the base peak among the aglycon product ions, *m/z* 153 ($^{1,3}A^+$) is some 7% of the base peak of the product ion mass spectrum. The complementary $^{1,3}B^+$ ion at *m/z* 135 is observed

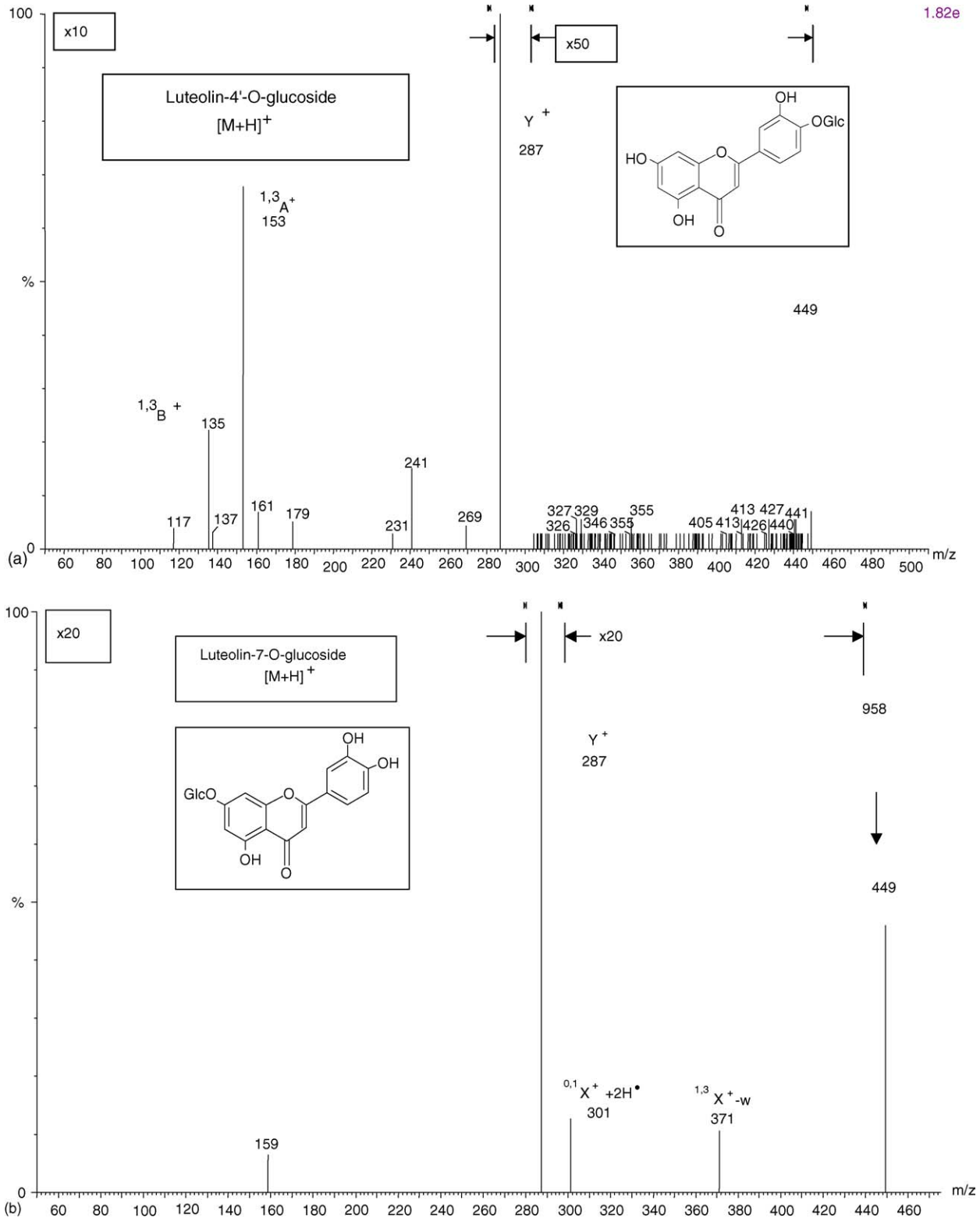

Fig. 3. Product ion mass spectra of $[M+H]^+$ (m/z 449) from (a) luteolin-4′-O-glucoside and (b) luteolin-7-O-glucoside.

also. Fragmentation of the Y^+ ion of luteolin-4′-O-glucoside is similar to that of the Y^+ ion of genistein-7-O-glucoside, shown in Scheme 7, except that the loss of a single CO molecule from the Y^+ ion of luteolin-4′-O-glucoside (to form m/z 259) is not observed. As discussed above, losses observed from the glucose moiety of the 7-O isomer were of 78 and 148 Da to form $^{1,3}X^+$–w and $^{0,1}X^+ + 2H^\bullet$ ions of m/z 371 and 301, respectively.

Table 4
Neutral losses observed (√) in glucose fragmentation of $[M–H]^-$ ions of deprotonated homoorientin, vitexin and orientin

	1–2 H_2O	48 Da[a]	3 H_2O	60 Da $^{0,4}X^-$[b]	66 Da $^{1,2}X^- – 2w$	76 Da[c]	78 Da $^{0,4}X^- – w$[d]	90 Da $^{0,3}X^-$[e]	106 Da[c]	108 Da $^{0,3}X^- – w$[f]	120 Da $^{0,2}X^-$	122 Da $^{0,2}X^- – 2H^\bullet$	136 Da $^{0,2}X^- – w + 2H^\bullet$	138 Da $^{0,2}X^- – w$	148 Da $^{0,1}X^- + 2H^\bullet$	149 Da $^{0,1}X^- + H^\bullet$	150 Da $^{0,1}X^-$	162 Da Y^-	163 Da $Y^- – H^\bullet$
Homo-orientin	√	√	√	√	√	√	√	√	√	√	√	√	√	–	√	√	√	√	√
Vitexin	–	–	–	–	√	–	√	√	–	√	√	√	–	√	√	–	–	√	√
Orientin	–	–	√	–	–	–	√	√	√	√	√	√	√	√	√	√	√	√	√

[a] Loss of the elements of $CH_2O + H_2O$.
[b] $^{0,4}X^-$ or $^{1,3}X^-$ or $^{2,4}X^-$.
[c] Unknown.
[d] $^{0,4}X^- – w$ or $^{1,3}X^- – w$ or $^{2,4}X^- – w$.
[e] $^{0,3}X^-$ or $^{1,4}X^-$.
[f] $^{0,3}X^- – w$ or $^{1,4}X^- – w$.

4.4. Comparison of two isomer pairs, apigenin-7-O-glucoside with apigenin-8-C-glucoside (vitexin) and luteolin-7-O-glucoside and luteolin-8-C-glucoside (orientin)

These compounds are compared with respect to fragmentation of each of $[M–H]^-$ and $[M + H]^+$. The product ion mass spectra of $[M–H]^-$ of apigenin-7-O-glucoside and of apigenin-8-C-glucoside (vitexin) are shown in Figs. 2(a) and 4(a), respectively; those of $[M–H]^-$ of luteolin-7-O-glucoside and luteolin-8-C-glucoside (orientin) are shown in Figs. 2(d) and 4(b), respectively.

4.4.1. Primary fragmentation of $[M–H]^-$

While the primary fragmentations of $[M–H]^-$ from apigenin- and luteolin-7-O-glucosides are losses of 163 and 162 Da to form $(Y–H)^{\bullet -}$ and Y^- ions, respectively, the primary fragmentation of $[M–H]^-$ from both vitexin and orientin is by cross-ring cleavage to form the $^{0,2}X^-$ ions of *m/z* 311 and 327, respectively. Only the $[M–H]^-$ ion from luteolin-7-O-glucoside (Fig. 2(d)) shows virtually no fragmentation of the glucose moiety and extensive fragmentation of the aglycon, whereas the $[M–H]^-$ ions of the other three compounds (apigenin-7-O-glucoside, apigenin-8-C-glucoside (vitexin), and luteolin-8-C-glucoside (orientin)) exhibit substantial fragmentation of the glycan and virtually none of the aglycon. In addition to the base peak due to the $^{0,2}X^-$ ion, vitexin shows (Fig. 4(a)) the $^{0,1}X^- + 2H^\bullet$ ion (*m/z* 283) together with $^{0,3}X^-$, $^{0,3}X^- – w$, and Y^- ions at *m/z* 341, 323, and 269, respectively. In addition to the $^{0,2}X^-$ base peak, orientin shows (Fig. 4(b)) extensive fragmentation of the glycan to form $[M–H–3w]^-$ (*m/z* 393); $^{1,3}X^- – w$ (*m/z* 369); $^{0,3}X^-$ (*m/z* 357); $^{0,3}X^- – w$ (*m/z* 339); $^{0,1}X^- + 2H^\bullet$ (*m/z* 299); $^{0,1}X^- + H^\bullet$ (*m/z* 298); $^{0,1}X^-$ (*m/z* 297); Y^- (*m/z* 285); and $(Y–H)^{\bullet -}$ (*m/z* 284). The neutral losses due to glycan cross-cleavage of the $[M–H]^-$ ion of vitexin and orientin are listed in Table 4.

The product negative ion mass spectra shown in Fig. 4(a) and (b) for vitexin and orientin, respectively, resemble those obtained by in-source CID and shown in Figs. 8 and 10(a), respectively, of Ref. [50]. Parenthetically, the product ion mass spectrum for $[M–H]^-$ of isovitexin (the 6-C-isomer of vitexin), shown in Fig. 10(b) of Ref. [50], is similar to that for vitexin as shown in Fig. 10(a) of Ref. [50]; virtually the sole difference is a three-fold increase in the relative intensity of the $^{0,3}X^-$ ion from isovitexin.

4.4.2. Primary fragmentation of $[M + H]^+$

The product ion mass spectra of $[M + H]^+$ from apigenin 8-C-glucoside (vitexin,) luteolin 8-C-glucoside (orientin) and luteolin-7-O-glucoside are shown in Figs. 3(b) and 5(a), (b), respectively; that of $[M + H]^+$ from apigenin-7-O-glucoside, obtained over the collision energy range of 10–50 eV, is not shown because only two product ions, Y^+ and $^{1,3}A^+$ (*m/z* 153), were observed. The product ion mass spectrum of protonated vitexin (Fig. 5(a)) differs considerably from that of apigenin-7-O-glucoside in that it shows extensive and intensive losses from the glycan (Table 5). The *m/z* 243 and 217 product ions are due to aglycon fragmentation.

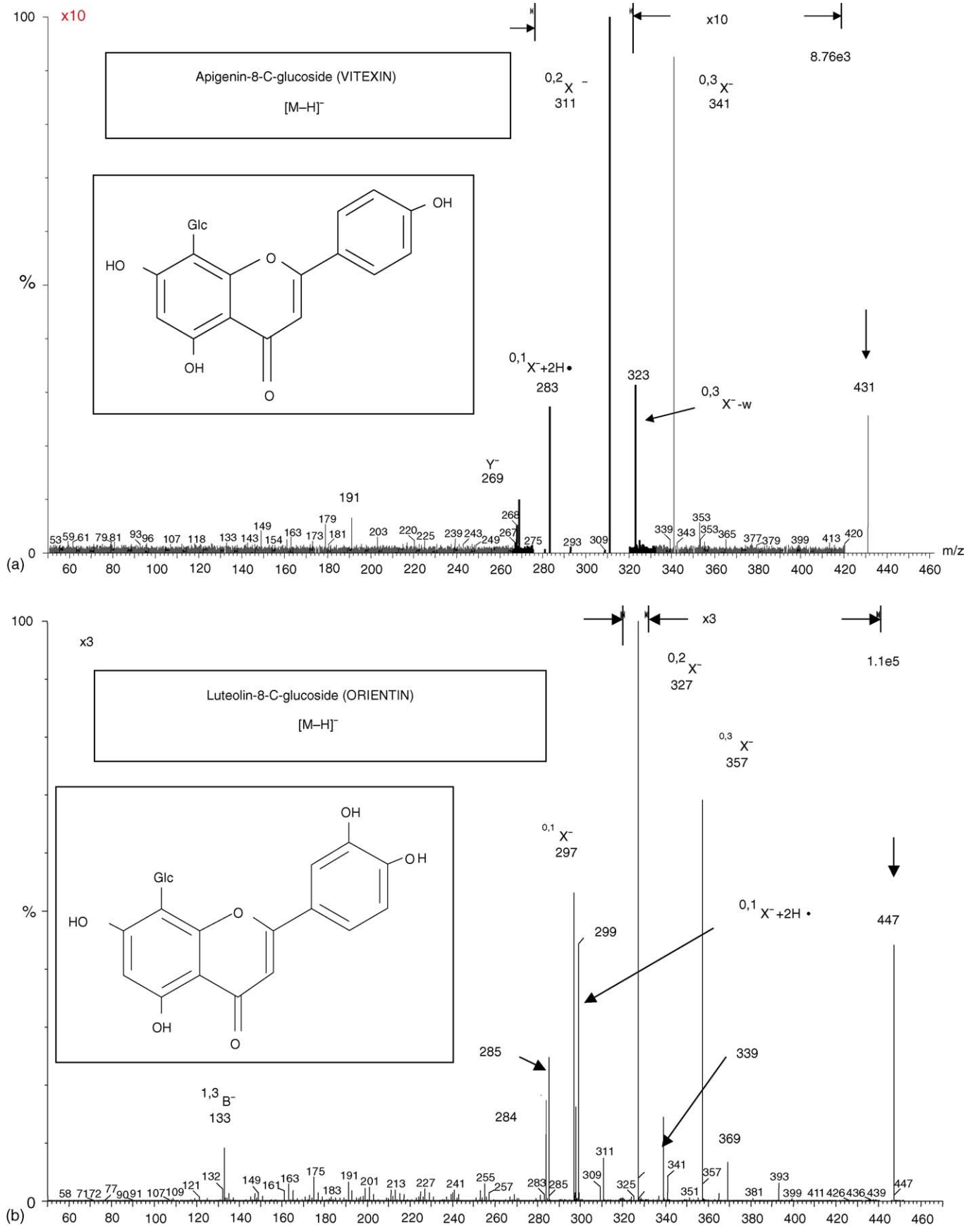

Fig. 4. Product ion mass spectra: (a) of $[M–H]^-$ (m/z 431) from apigenin-8-C-glucoside (vitexin); (b) of $[M–H]^-$ (m/z 447) from luteolin-8-C-glucoside (orientin).

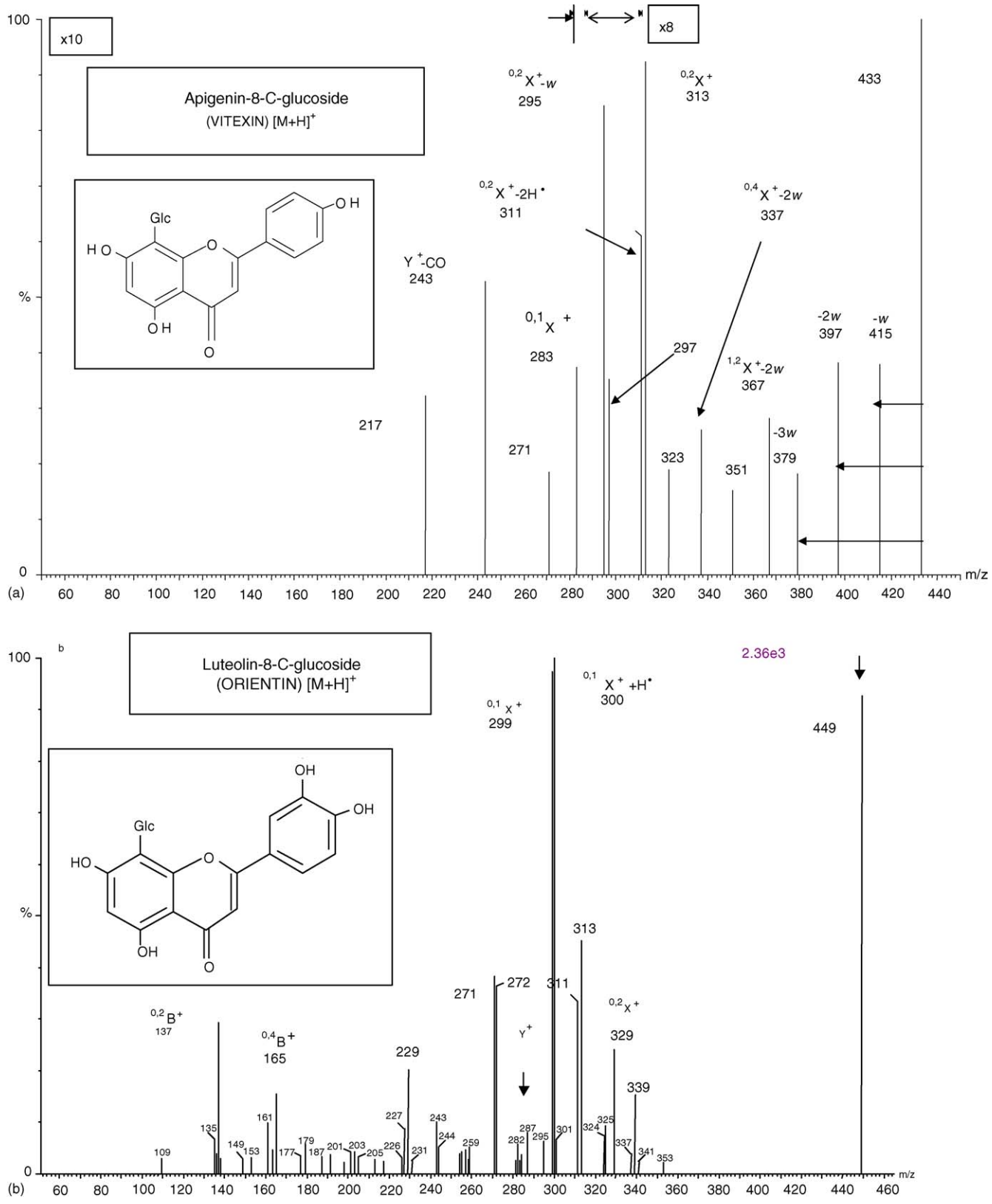

Fig. 5. Product ion mass spectra: (a) of $[M + H]^+$ (m/z 433) from apigenin-8-C-glucoside (vitexin); (b) of $[M + H]^+$ (m/z 447) from luteolin-8-C-glucoside (orientin).

The principal product ion from luteolin-7-O-glucoside (Fig. 3(b)) is Y^+. Minor losses of 78 and 148 Da were observed, as shown in Table 2, to form the $^{1,3}X^+–w$ (m/z 371) and $^{0,1}X^+ + 2H^\bullet$ (m/z 301) ions, respectively, together with an aglycon product ion of m/z 159. The product ion mass spectrum of $[M + H]^+$ from orientin (Fig. 5(b)) shows extensive fragmentation of both the glycan (Table 5) and the aglycon. However, fragmentation of the glycan is restricted to neutral losses of

Table 5
Neutral losses observed (√) in glucose fragmentation of $[M+H]^+$ ions of protonated homoorientin, vitexin and orientin

	1–3 H_2O	66 Da $^{1,2}X^+-2w$	72 Da $^{1,2}X^+-4w$	82 Da[a]	84 Da $^{1,2}X^+-3w$	96 Da $^{0,4}X^+-2w$[b]	108 Da $^{0,3}X^+-w$[c]	110 Da[a]	112 Da[a]	120 Da $^{0,2}x^+$	122 Da $^{0,2}X^+-2H^\bullet$	124 Da[a]	125 Da[a]	136 Da[a]	138 Da $^{0,2}X^+-w$	148 Da $^{0,1}X^+ + 2H^\bullet$	149 Da $^{0,1}X^+ + H^\bullet$	150 Da $^{0,1}X^+$	162 Da Y^+
Homo-orientin	√	√	√	√	√	√	–	√	–	√	–	√	–	–	√	–	–	√	√
Vitexin	√	√	–	√	–	√	–	√	–	√	√	–	–	√	√	–	–	√	√
Orientin	–	–	–	–	–	√	√	√	√	√	–	√	√	√	√	√	√	√	√

[a] Unknown.
[b] $^{0,4}X^+-2w$ or $^{1,3}X^+-2w$ or $^{2,4}X^+-2w$.
[c] $^{0,3}X^+-w$ or $^{1,4}X^+-w$.

≥96 Da. The *m*/*z* 339 product ion observed from protonated orientin is due to B-ring cleavage with the loss of 110 Da; similar losses of 110 Da were observed from protonated homoorientin and vitexin. Such cleavages are relatively rare in flavonoid glucosides.

4.5. Comparison of the product ion mass spectra of three C-glucosides

In contrast to the fragmentations exhibited by protonated and deprotonated O-glycosides, the corresponding C-glycosides (luteolin-6-C-glucoside (homoorientin), apigenin-8-C-glucoside (vitexin) and luteolin-8-C-glucoside (orientin)) exhibited fragmentation of the glycan usually with the loss of neutral moieties of mass <162 Da together with fragmentation of the flavonoid moiety bonded to a residual part of the glycan. The variety of fragmentation pathways of the glycan in 6-C- and 8-C-flavonoids appears to be virtually compound specific for the flavonoid-C-glycosides examined to date.

4.5.1. Deprotonated homoorientin, vitexin and orientin

The product ion mass spectra of $[M–H]^-$ from homoorientin, vitexin and orientin and shown in Figs. 4(a), (b) and 6, respectively, were obtained at a collision energy of 46–47 eV. The product ion mass spectrum of $[M–H]^-$ from homoorientin (Fig. 6) is remarkably similar to that shown in Fig. 7 of Ref. [50]. Major fragmentation pathways for $[M–H]^-$ ions involve cleavage of the O–C(1) bond in the glycan such that the base peak in the product ion mass spectra of deprotonated homoorientin, vitexin and orientin is $^{0,2}X^-$; other major features are $^{0,1}X^- + 2H^\bullet$, $^{0,1}X^- + H^\bullet$, $^{0,1}X^-$, and $^{0,3}X^-$ ions from homoorientin and orientin, and $^{0,1}X^- + 2H^\bullet$ from vitexin. The neutral losses observed from $[M–H]^-$ of homoorientin, vitexin and orientin are shown in Table 4. Deprotonated homoorientin exhibits the highest number of neutral losses. The Y^- and $(Y–H)^{\bullet -}$ ions were observed in each case though of low ion signal intensity.

A breakdown curve for deprotonated homoorientin, *m*/*z* 447, obtained over the collision energy range of 1–24 eV, is shown in Fig. 7(a)–(c). In Fig. 7(a), the precursor ion signal intensity increases initially due to enhanced ion transmission efficiency with increasing collision energy. For collision energy >5 eV, the precursor ion signal intensity decreases due to fragmentation. The product ion signal intensity curves show pronounced tailing to low collision energy indicating that the energy resolution of the precursor ion beam is low; thus, precise product ions appearance energies were not obtained. $^{0,2}X^-$ (*m*/*z* 327) and either $^{0,3}X^-$ or $^{1,4}X^-$ (*m*/*z* 357), formed by cross-cleavage, dominate over the entire collision energy range.

Chemical computations using the PM3 method were carried out of the structures of deprotonated homoorientin with proton loss from each of the 3′- and 4′-hydroxyl groups; the structures are shown in Scheme 9(a) and (b), respectively. The structure with deprotonation at the 3′-hydroxyl shows both strong H-bonding (between the glycan O atom and the H atom of the C(7) hydroxyl group) and inclination of the plane of the B-ring by some 36° to that [31] of the A and C rings (Scheme 9(a)). This structure does not permit resonance structures. The struc-

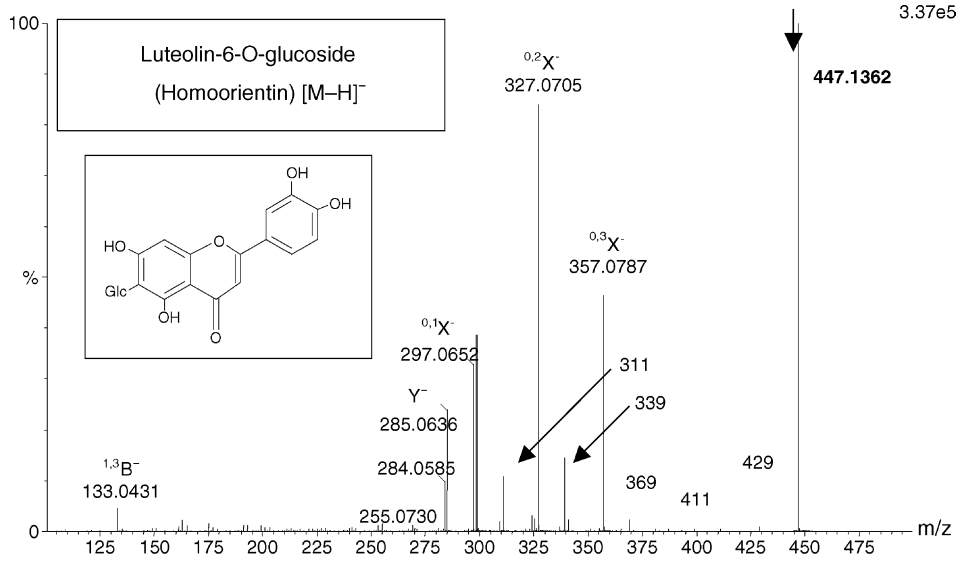

Fig. 6. Product ion mass spectrum of $[M–H]^-$ (m/z 447) from homoorientin (luteolin-6-C-glucoside).

ture of Scheme 9(b) differs markedly from that of Scheme 9(a) in that an additional strong H-bond is formed between the H atom attached to C(2) of the glycan and the O atom at C(5) of the A-ring. This latter H-bond is facilitated by the resonance that allows the negative charge to migrate to the keto oxygen of the C-ring, as shown in Scheme 9(b). The combined effect of the C-glycosidic bonding supplemented by two strong hydrogen bonds (as judged by the O···H bond length in each case) and the resonance structure that creates an ethylenic linkage between C and B rings is to shrink the ion and to bring about coplanarity of the B-ring with the A and C rings. There is a loss of entropy (and increase in enthalpy) in what may be an example of cooperative interactive bonding; such positive cooperativity arises when the dynamic motion of the central chain is reduced by the formation of H-bonds [67,68]. The net effect is to increase activation energies for fragmentation of both the aglycon and cleavage of the glycan to form the Y^- ion. Thus, upon CID, fragmentation by cross-cleavage of the glycan is preferred. Each cross-cleavage requires rupture of one of the H bonds shown in Scheme 9.

In Fig. 7(b) are shown product ion data on an expanded (or zoom) scale; the precursor ion curve has been omitted and the $^{0,2}X^-$ and either $^{0,3}X^-$ or $^{1,4}X^-$ product ion curves have been curtailed at 10 eV. The m/z 429 product ion curve, formed by loss of H_2O, goes through a maximum and decreases at collision energies in excess of 17 eV indicating that competing ring-cleavage processes overtake the H_2O loss by incorporating H_2O into the neutral fragment lost. The other major product ions observed and shown in Fig. 7(b) are, in decreasing order of ion signal intensity at a collision energy of 24 eV, $^{0,1}X^-$ (m/z 297), Y^- (m/z 285), $^{0,3}X^-$–w or $^{1,4}X^-$–w (m/z 339), and $^{0,1}X^- + 2H$ (m/z 299). The increase in ion signal intensity with collision energy of either $^{0,3}X^-$–w or $^{1,4}X^-$–w (or both) of m/z 339 parallels the decrease in m/z 429 and supports the above explanation for this behavior.

In Fig. 7(c) are shown data on a further expanded (or zoom) scale of minor product ion species. The curves are of two types; those that increase linearly with collision energy and those that exhibit a maximum. At a collision energy of 17 eV, there is a cross-over point at which the ion signal intensities of the precursor ion and the most abundant product ion species ($^{0,2}X^-$) are equal. At this point, all of the product ion curves are increasing and, to a first approximation, the order of the product ions in terms of decreasing ion signal intensity at a collision energy of 17 eV corresponds to the order of the appearance energies of the product ions. Thus the product ions, arranged in order of increasing appearance energy, are $^{0,2}X^-$, $^{0,3}X^-$, $[M–H–w]^-$, Y^-, $^{0,4}X^-$–w, $^{0,3}X^-$–w, $^{0,1}X^-$, $[M–H–2w]^-$, $[M–(CH_2O + H_2O)]^-$, $^{0,4}X^-$, $^{0,2}X^-$–$2H^\bullet$, $^{0,1}X^- + 2H^\bullet$, m/z 371 (−76 Da), m/z 341 (−106 Da), $[M–H–3w]^-$, $^{0,2}X^-$–$w + 2H^\bullet$, and $^{1,2}X^-$–$2w$.

4.5.2. Protonated homoorientin, vitexin and orientin

The principal glycan-cleavage ions observed from $[M + H]^+$ of homoorientin, vitexin and orientin are shown in Table 5. The product ion mass spectrum of $[M + H]^+$ (m/z 449) from homoorientin (luteolin-6-C-glucoside) is shown in Fig. 8; those from vitexin and orientin are shown in Fig. 5(a) and (b), respectively. Homoorientin and orientin are isomeric yet they can be distinguished readily by their product ion mass spectra; the base peak for homoorientin is $^{0,1}X^+$ (m/z 299) whereas for orientin $^{0,1}X^+$ and $^{0,1}X^+ + H^\bullet$ (m/z 300) are base peaks of equal ion signal intensity. The proposed major fragmentation pathways for $[M + H]^+$ ions [23] involve cleavage of the O–C(1) bond in the glycan such that the base peak in the product ion mass spectra of protonated homoorientin and orientin is $^{0,1}X^+$; the base peak in the product ion mass spectrum of protonated vitexin was $^{0,2}X^+$. In the mass spectra of protonated homoorientin, vitexin, and orientin obtained by FAB [23], $^{0,2}X^+$ was the major product ion. The product ion mass spectrum of $[M + H]^+$ for orientin is characterized by myriad product ions of mass/charge ratio $\leq$353, as shown in Fig. 5(b). In Table 5, it is seen that homoorientin exhibits a wide range of neutral losses from the glycan while orientin exhibits losses of $\geq$96 Da only. Some of the losses shown in Table 5 have not been identified. Y^+ (m/z 287) from homoorientin was observed with low ion signal intensity (as was the

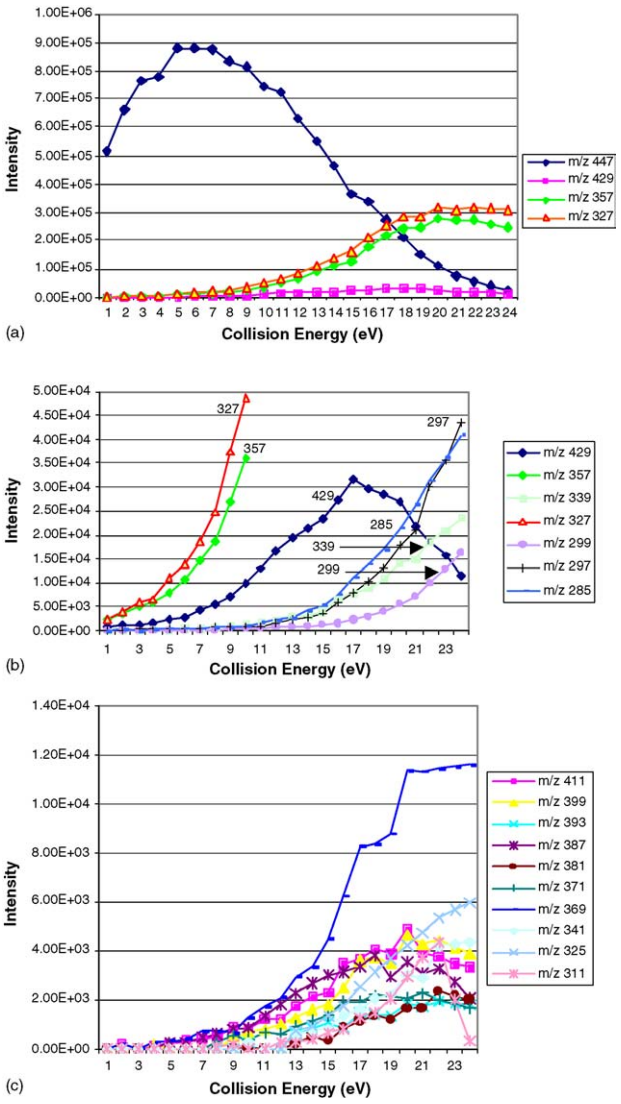

Fig. 7. Breakdown graph of $[M–H]^-$ (m/z 447) from homoorientin: (a) principal product ions; (b) major product ions shown with an intensity scale expanded 20-fold; and (c) minor product ions shown with an intensity scale expanded approximately 70-fold.

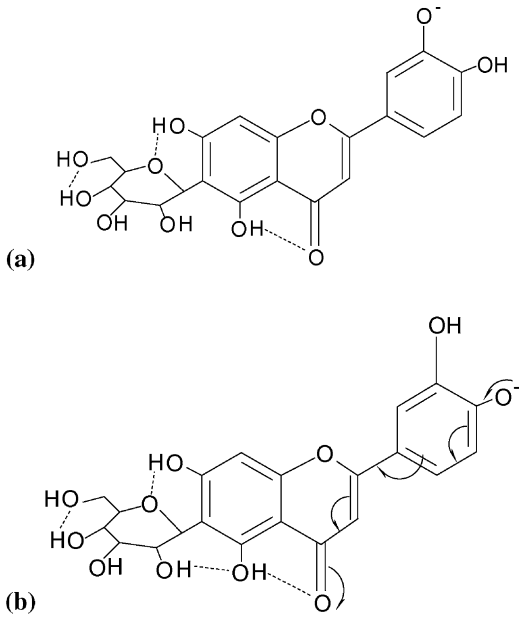

Scheme 9. Calculated structures for deprotonated homoorientin (luteolin-6-C-glucoside) $[M–H]^-$: (a) deprotonated at the 3′-position; and (b) deprotonated at the 4′-position.

isomeric Y^+ from orientin) and virtually no aglycon fragmentation was observed from homoorientin.

The interesting observation of m/z 271 and 272, of high and equal relative ion signal intensity in Fig. 5(b), can be explained most readily by the loss of a CO molecule from each of $^{0,1}X^+ + H$ (m/z 300) and $^{0,1}X^+$ (m/z 299), respectively. The product ions of m/z 271 and 272 from protonated orientin are the first observed examples of ions that have been formed by neutral losses of part of the glycan and part of the flavonoid. In addition, the $^{0,2}B^+$ and $^{0,4}B^+$ ions of m/z 137 and 165, respectively, were observed.

A breakdown curve is shown in Fig. 9(a) for seven product ions from protonated homoorientin, m/z 449, over the collision energy range of 6–24 eV. The data for collision energies <6 eV are omitted. Each of the curves due to losses of 1–3 water molecules, that is, m/z 431, 413, and 395, together with $^{1,2}X^+–2w$ (m/z 383), exhibits a maximum at 16 ± 3 eV. This behavior indicates that the corresponding neutral losses are subsumed by other neutral entities of greater mass at higher collision energies. The three major product ions observed at a collision energy of 24 eV are, in order of decreasing ion signal intensity, $^{0,1}X^+$ (m/z 299), $^{0,2}X^+$ (m/z 329), and $^{0,4}X^+–2w$ (m/z 353). Glycan cross-ring cleavage involving the O–C(1) bond is prevalent, as for the fragmentation of deprotonated homoorientin but, unlike the fragmentation of deprotonated homoorientin, 0,3-cleavage is not observed for protonated homoorientin.

In Fig. 9(b) are shown product ion data for seven product ions further on an expanded (×6) scale; the curve for m/z 431 has been repeated as a reference curve. The three dominant product ion species over the collision energy range 19–23 eV are due to loss of 4w (m/z 377), B-ring scission (m/z 339), and formation of $^{1,2}X^+–3w$ (m/z 365). Of the four product ions remaining, m/z 325 is of unknown identity, m/z 287 is Y^+, m/z 311 is $^{0,2}X^+–w$, and m/z 367 is due to the loss of the elements of ethanol and two water molecules. As expected for flavonoid-C-glycosides, $^{0,2}X$-type ions at m/z 311 and 313 (negative and positive ion mass spectra, respectively,) were observed rather than Y-type ions.

In a positive ion FAB/MS/MS study of 6-C- and 8-C-glycoside flavonoids, Claeys and co-workers [23] have tabulated percentages of total product ion yield for major product ions from $[M + H]^+$ ions of vitexin, isovitexin, orientin, and homoorientin. Product ion mass spectra were obtained by linked scanning at constant B/E. Given that the collision energy "was lower than 30 eV" [23], as compared with a collision energy of 46–47 eV used in this work, the product ion mass spectra obtained by linked scanning are substantially similar to those reported in this work in that multiple glycan cross-cleavages were observed. Nevertheless, a comparison of Table 5 with Table 1 of Ref. [23] shows some systematic differences in the neutral losses observed. These systematic differences may be due to one or more of the disparity in collision energies, internal excitation

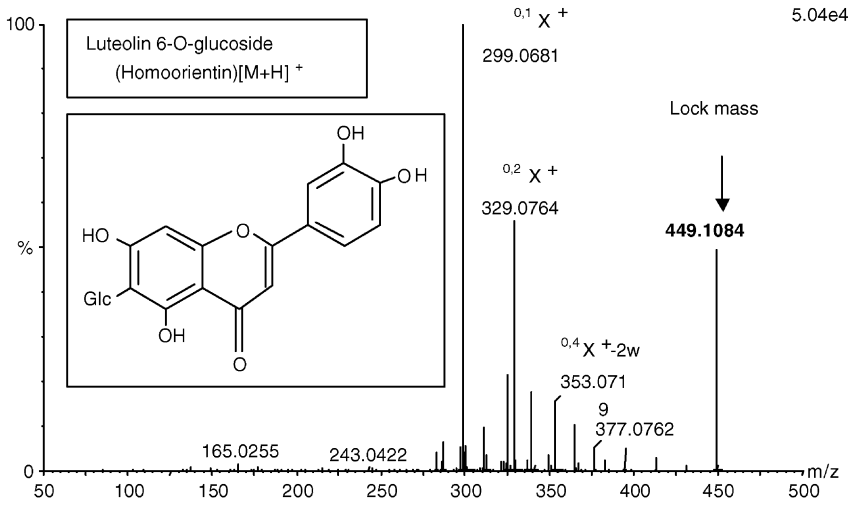

Fig. 8. Product ion mass spectrum of $[M + H]^+$ (m/z 449) from Homoorientin (luteolin-6-C-glucoside). Experimental conditions: cone voltage, 35 V; capillary voltage, 3 kV; collision energy, 4 eV for 1 min, 46 eV for 18 min.

of protonated molecules produced by FAB, and poor parent ion resolution in linked scanning at constant B/E. Claeys and coworkers show a FAB product ion mass spectrum of protonated orientin (Fig. 2 in Ref. [23]) where the ion relative intensities vary markedly from those obtained by linked scanning; however, the FAB product ion mass spectrum is in qualitative agreement with that obtained by ESI at a collision energy of 24 eV (not shown).

4.6. Summary of analytical distinguishing features

The analytical objectives of this work were to acquire product ion mass spectra for flavonoid glycosides in support of LC/MS/MS analysis, to identify the position of glycoside attachment so as to distinguish between 3-O-, 7-O-, and 4′-O-glycosidic flavonoids, to differentiate between O- and C-glycosides, and to examine cleavage across the glucose ring. From inspection of the observed product ion mass spectra, it is possible to discern several analytical distinguishing features that permit identification of all of the flavonoid glycosides that have been examined. The distinguishing features are presented in Table 6.

4.7. Chemical computations

Using the semiempirical PM3 method, a number of relatively crude chemical computations have been carried out of luteolin glucosylated in turn at the 3′-, 4′-, 6-, 7-, and 8-positions. Luteolin glucosides were selected because the product ion mass spectra of protonated and deprotonated luteolin glucosylated in turn at the 4′-, 6-, 7-, and 8-positions have been discussed above. All of the fifteen protonated, neutral, and deprotonated luteolin glucosides examined are isoelectronic. In addition, chemical computations were made of neutral glucose and luteolin. The calculations were obtained in order to explore the relationship between the calculated structures together with intramolecular H-bond formation and the observed product ion mass spectra. Six further computations were carried out using the ab initio DFT method on protonated and deprotonated luteolin glucosylated in turn at the 6-, 7-, and 8-positions. In Fig. 10(a) and (b) are shown the PM3-calculated structures of neutral glucose and neutral luteolin, respectively. The dashed line in Fig. 10(a) represents an H-bond in that the distance between the H atom of the C(4) hydroxyl group and the O atom of the CH_2OH group at C(5) is ∼1.8 Å. Formation of this glucose intramolecular H-

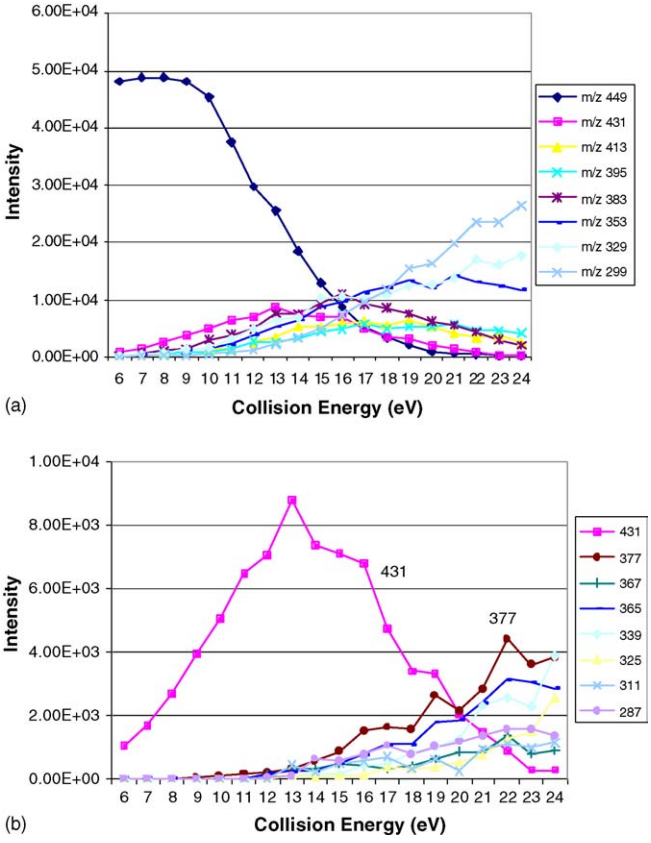

Fig. 9. Breakdown graph of $[M + H]^+$ (m/z 449) from homoorientin: (a) principal product ions; and (b) minor product ions shown with an intensity scale expanded six-fold.

Table 6
Summary of distinguishing mass spectrometric features that permit identification of all of the 12 flavonoid glycosides examined

Compound(s)	Precursor ion	Distinguishing feature(s) from product ion mass spectra
Quercitin-3-O-galactoside Quercitin-3-O-glucoside	$[M+H]^+$ isomers	*3-O-Galactoside*: $B^+–H_2O$ (*m*/*z* 145) *3-O-Glucoside*: no *m*/*z* 145
Quercitin-3-O-galactoside Quercitin-3-O-glucoside	$[M–H]^-$ isomers	Distinguishable by product ion mass spectra; *galactoside and 3-O-glucoside* have only two common product ions, *m*/*z* 271 ($–CH_2O$) and 255 ($–(H_2O+CO)$); no glycan fragmentation
Kaempferol-3-O-glucoside Kaempferol-7-O-glucoside	$[M–H]^-$ isomers	*3-O-glu*: Y^-, $(Y–H)^{\bullet -}$ ions plus *m*/*z* 255 and 227 *7-O-glu*: Y^-, $(Y–H)^{\bullet -}$ ions plus *m*/*z* 257 and 151 ($^{1,3}A^-$) Minor fragmentation of the glycan for both 3-O-glu and 7-O-glu
7-O-glucosides of isomers (apigenin + genistein) plus luteolin, naringenin	$[M+H]^+$	Of the four *7-O-glucosides* examined, only genistein exhibited extensive fragmentation of both aglycon and glycan; see Table 2
Genistein-7-O-glucoside Luteolin-7-O-glucoside	$[M+H]^+$	Glycan fragmentations are strictly complementary
Apigenin-7-O-glucoside Naringenin-7-O-glucoside	$[M+H]^+$	No glycan fragmentations
Naringenin-7-O-glucoside	$[M–H]^-$	Y^- ion (*m*/*z* 271) only; no $(Y–H)^{\bullet -}$ ion
Luteolin-7-O-glucoside Luteolin-4′-O-glucoside	$[M–H]^-$ isomers	*7-O*: Y^- and $(Y–H)^{\bullet -}$ ions plus extensive aglycon fragmentation; no glycan fragmentation. C(3′) OH inhibits glycan 0,2 cleavage from $[M–H]^+$ and $[M–H]^-$. Base peak is $^{1,3}B^-$ ion *4′-O*: Y^- ion only; no $(Y–H)^{\bullet -}$ ion. Base peak is $^{1,3}B^-$ ion. $^{0,2}X^-$ ion
7-O-glucosides of isomers (apigenin + genistein), (kaempferol + luteolin), naringenin	$[M–H]^-$	Distinguishable by glycan fragmentation; see Table 3
Apigenin-7-O-glucoside Apigenin-8-C-glucoside Genistein-7-O-glucoside	$[M–H]^-$ isomers	*Apigenin-7-O-glu*: $(Y–H)^{\bullet -}$ ion is base peak; Y^- ion is ∼80% base peak *8-C-glu*: $^{0,2}Y^-$ ion is base peak; $^{0,1}Y^-–2H$ ion is ∼35% base peak *Genistein-7-O-glu*: $(Y–H)^{\bullet -}$ ion is base peak; Y^- ion is ∼80% base peak; shows $^{0,2}X^-$ ion only; no aglycon fragmentation
Apigenin-7-O-glucoside Apigenin-8-C-glucoside Genistein-7-O-glucoside	$[M+H]^+$ isomers	*Apigenin-7-O-glu*: Y^+ and $^{1,3}A^+$ ions *8-C-glu*: weak Y^+ and extensive and intensive glycan fragmentations *Genistein-7-O-glu*: base peak, Y^+; extensive glycan fragmentation
Luteolin-6-C-glucoside Luteolin-8-C-glucoside	$[M–H]^-$ isomers	Distinguishable by glycan fragmentation variety, see Table 4 *6-C*: base peak, $^{0,2}X^-$; $^{0,3}X^-$ (or $^{1,4}X^-$) ion is ∼56% base peak *8-C*: base peak, $^{0,2}X^-$; $^{0,3}X^-$(or $^{1,4}X^-$) ion is ∼24% base peak
Luteolin-6-C-glucoside Luteolin-8-C-glucoside	$[M+H]^+$ isomers	Distinguishable by glycan fragmentation variety, see Table 5 *6-C*: wide mass range of neutral losses from glycan *8-C*: neutral losses of ≥96 Da only

bond completes a six-membered ring such that glucose takes on a bicyclic structure. In the luteolin structure shown in Fig. 10(b), there are two points of interest to note: first, an intramolecular H-bond is formed between the hydroxyl H atom at C(5) of the A-ring and the keto-O atom of the C-ring to complete a six-membered ring and, second, the dihedral angle defined by the ether oxygen of the C-ring, C(2) of the C-ring, and C(1′) and C(2′) of the B-ring is 46°. The intramolecular H-bond inhibits substitution of the hydroxyl H atom at C(5) thus 5-O-glucosides are rare. The positive value of the angle of inclination of the B-ring with respect to the coplanar A and C rings indicates that the 3′-OH lies above the plane of the A and C rings.

The structure of luteolin-3′-O-glucoside protonated at the keto-oxygen of the C-ring exhibits the H-bonds as in luteolin and glucose and another between the ring O atom of glucose and the hydroxyl H atom at C(4′); the O–C(2)–C(1′)–C(2′) dihedral angle is but 1°, thus the A, B, and C rings of the luteolin moiety are essentially coplanar. The structure of neutral luteolin-3′-O-glucoside exhibits three H-bonds also, and the O–C(2)–C(1′)–C(2′) dihedral angle is 46°, that is, unchanged from neutral luteolin. Thus 3′-O-glucosylation of luteolin has no effect upon the orientation of the B-ring with respect to the A and C rings. The structure of luteolin-3′-O-glucoside deprotonated at C(7) is similar to that of the neutral counterpart in that it exhibits three H-bonds and the dihedral angle is unchanged at 46°.

For the computed isoelectronic structures of protonated, neutral, and deprotonated luteolin-4′-O-glucoside, protonation occurs on the keto-oxygen of the C-ring and deprotonation occurs at C(7). H-bond formation was maximised upon deprotonation at C(7) whereas deprotonation at each of C(3′) and C(5) would lead to the loss of a H-bond. The structures for the 4′-O-glucoside are essentially similar to the corresponding structures for the 3′-O-glucoside, except for the attachment position of the glucose moiety and a H-bond is formed between the ring O atom of glucose and the hydroxyl H atom at the C(3′)

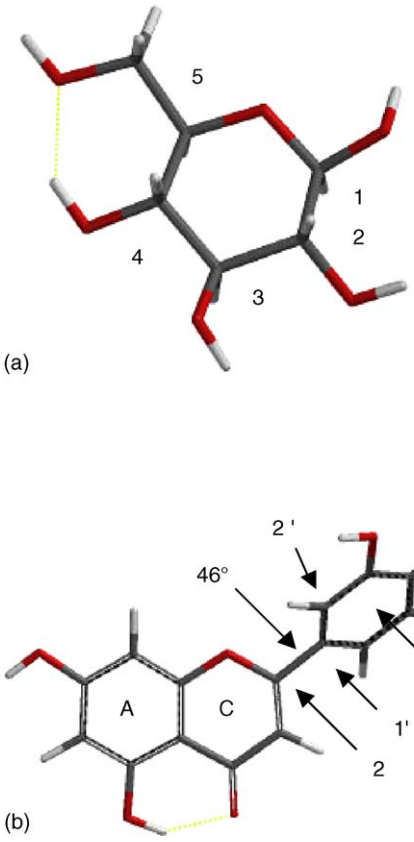

Fig. 10. Computed structures of (a) glucose; and (b) luteolin. The hydrogen bond in glucose is designated by a green dotted line. The dihedral angle O–C(2)–C(1′)–C(2′) of 46° is indicated by an arrow.

rather than C(4′). While the O–C(2)–C(1′)–C(2′) dihedral angle for neutral luteolin-4′-O-glucoside is 46°, as was the case for neutral luteolin and neutral luteolin-3′-O-glucoside, the dihedral angles for protonated and deprotonated molecules are 2 and 0°, respectively. The B-ring in deprotonated luteolin-4′-O-glucoside is now coplanar with the A and C rings.

The product ion mass spectrum of protonated luteolin-4′-O-glucoside (Fig. 3(a)) showed principally Y^+ product ion. Despite the calculated additional H-bond between the glucose and luteolin moieties, cleavage of the glycan to form Y^+ was not accompanied by cross-ring cleavages of the glycan. Similarly, $[M–H]^-$ of luteolin-4′-O-glucoside fragments principally to Y^- only (*m*/*z* 285), despite the additional H-bond between the glucose and luteolin moieties. This additional H-bond appears to be entirely ineffective in directing fragmentation of protonated and deprotonated luteolin-4′-O-glucoside so that the product ion mass spectra of $[M + H]^+$ and $[M–H]^-$ are remarkably similar to their counterparts for luteolin-7-O-glucoside for which (see below) there is no computed additional H-bond between the glucose and luteolin moieties.

The structures for protonated, neutral, and deprotonated luteolin-7-O-glucoside computed by PM3 are shown in Fig. 11; the corresponding structures for luteolin-6-C-glucoside are shown in Fig. 12. The corresponding structures for luteolin-8-C-glucoside are not shown but structural details are given in Table 7. For each of these three isomeric compounds, pro-

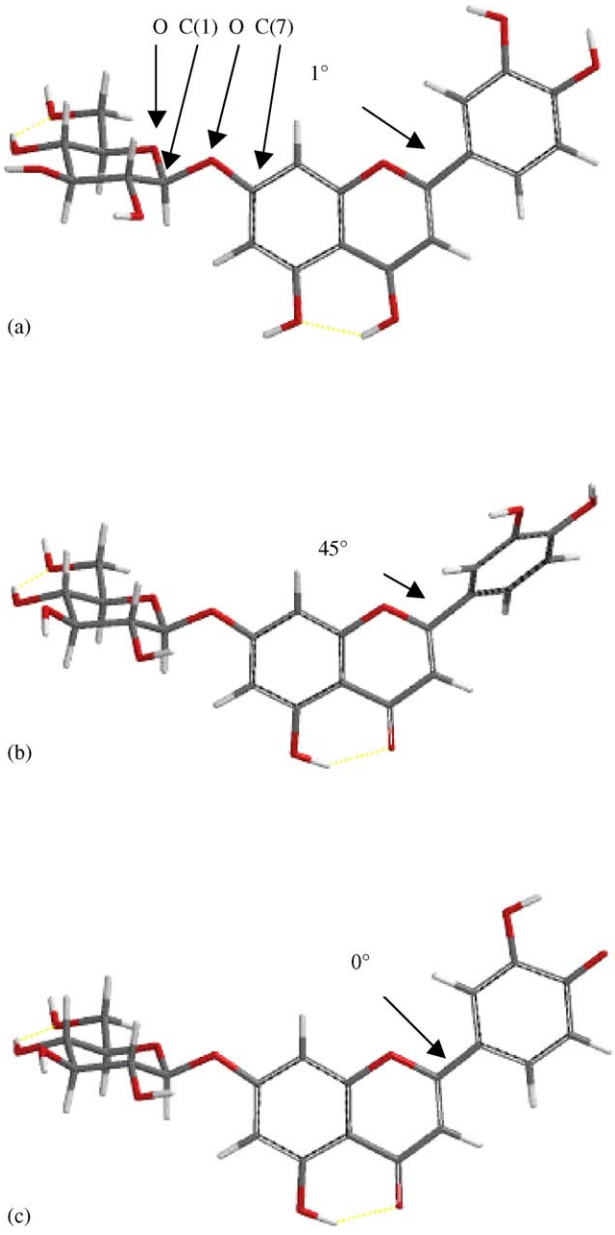

Fig. 11. Computed structures of luteolin-7-O-glucoside: (a) protonated; (b) neutral; (c) deprotonated. The arrow indicates the dihedral angle for B-ring twist.

tonation occurs at the keto-oxygen of the C-ring as shown in Fig. 11(a), while deprotonation occurs at C(4′) (Fig. 11(c)) so as to enhance resonance within the structure of the negatively-charged ion, as discussed above for homoorientin-6-C-glucoside (Scheme 9). The structures for each of six ion species obtained using PM3 and DFT methods are remarkably similar; so much so that tabulations of individual atom coordinates are obviated. The structures can be distinguished by both the dihedral angle at the bridge between the C and B rings (defined by the ether O atom of the C-ring, C(2) of the C-ring, and C(1′) and C(2′) of the B-ring) and by the dihedral angle at the bridge between the A-ring and the glycan; definition of the glycan twist angle varies with the type of substitution thus the definitions are given as footnotes to Table 7.

Table 7
Calculated values of the angle of inclination of the B-ring plane to that of the A and C rings (B-ring twist), and of the angle of inclination of the glycan to the plane of the A and C rings (glycan twist) for some glucosides of luteolin; semiempirical (PM3) and ab initio (DFT) methods were employed

Compound	PM3[a] B-ring twist[c] (°)	DFT[b] B-ring twist (°)	PM3 Glycan twist (°)	DFT Glycan twist (°)
$[M+H]^+$, luteolin-6-C-glucoside	1	2	107.6[d]	99.8
$[M+H]^+$, luteolin-7-O-glucoside	1	2.8	−84[e]	−101.8
$[M+H]^+$, luteolin-8-C-glucoside	−7	21.9	−81.9[f]	−87.1
$[M–H]^-$, luteolin-6-C-glucoside	0	0.2	135.7	158.6
$[M–H]^-$, luteolin-7-O-glucoside	0	1.0	−94.9	−95.4
$[M–H]^-$, luteolin-8-C-glucoside	−1	12.6	−74.8	−75.7
M, luteolin-6-C-glucoside	45	–	26.3	–
M, luteolin-7-O-glucoside	45	–	−103.8	–
M, luteolin-8-C-glucoside	45	–	42.6	–

[a] PM3, semiempirical method.
[b] Density functional theory (DFT) ab initio method.
[c] Angle of B-ring twist with respect to the plane of the A and C rings, O–C(2)–C(1′)–C(2′).
[d] Angle of glycan twist with respect to the plane of the A and C rings for 6-C, O–C(1)–C(6)–C(7).
[e] Angle of glycan twist with respect to the plane of the A and C rings for 7-C, O–C(1)–O–C(7).
[f] Angle of glycan twist with respect to the plane of the A and C rings for 8-C, O–C(1)–C(8)–C(7).

The results of the PM3 and DFT methods are compared in Table 7 with respect to the calculated values of the angle of inclination of the B-ring plane to that of the A and C rings (B-ring twist), and of the angle of inclination of the glycan to the plane of the A and C rings (glycan twist) for the 6-C-, 7-O-, and 8-C- glucosides of luteolin. The time-consuming ab initio DFT method was applied only to the structures of ionic species.

The negative sign for the B-ring twist in Table 7 indicates that the 3′-OH group lies below the plane of the A and C rings. The B-ring twist angles calculated by PM3 and DFT are generally in good agreement except for the single example of protonated 8-C-glucoside; although this dihedral angle of −7° differs slightly from those of the other protonated molecules examined, the same value was obtained regardless of the initial geometry assumed for the computation. The DFT value is 21.9°.

The positive and negative values for the glycan twist angle indicate that the glucose ring O atom lies either above or below the plane of the paper, respectively. Again, the agreement between the glycan twist angle calculated for each of the six species by each of PM3 and DFT is remarkably good. Not only do the results agree with respect to sign but the absolute values are similar. The glycan twist angle for 7-O- and 8-C-glucosides is generally of the order of $-90 \pm 16°$; however, those for 6-C-glucoside are positive and range from 107.6 to 158.6°. A rotation of the glucose plane through >180° in going from the 7-O- and 8-C- to the 6-C-glucoside indicates a uniqueness of the 6-C-glucoside among the isomers examined and, indeed, the structure of luteolin-6-C-glucoside is unique because the glucose-luteolin C–C bond is located adjacent to two hydroxylated positions in luteolin.

Each structure shown in Fig. 11 for luteolin-7-O-glucoside exhibits two H-bonds; H-bond formation is not observed between the glucose and luteolin moieties. The B-ring twist angles for protonated and deprotonated luteolin-7-O-glucoside indicate A-, C-, and B-ring coplanarity. The product ion mass spectrum of $[M+H]^+$ ions of luteolin-7-O-glucoside (Fig. 3(b)) showed principally Y^+, together with minor fragmentations of the glucose moiety to yield $^{1,3}X^+$–*w* and $^{0,1}X^+ + 2H^\bullet$ of *m*/*z* 371 and 301, respectively. From the structure shown in Fig. 11(a), it could be anticipated that in the absence of a H-bond between the glucose and luteolin moieties, facile scission of the glucoside C–O bond would lead to formation of Y^+, and that 1,2 and 1,3 cross-ring cleavages of the glucose moiety would be observed. In this case, only the latter cross-ring cleavage was observed. The product ion mass spectrum of $[M–H]^-$ of luteolin-7-O-glucoside showed only the loss of glycan with the formation of Y^- and $(Y–H)^{\bullet -}$ as shown in Fig. 2(d). Thus, in the absence of a glucose–luteolin H-bond, loss of the glycan is facile as would be expected from Fig. 11(c).

The structure for protonated luteolin-6-C-glucoside (homoorientin) shown in Fig. 12(a) exhibits the formation of an H-bond between the glucose and luteolin moieties (between the glucose ring O atom and the C(7) hydroxyl H atom) in addition to the two expected H-bonds. For the structures of the neutral and deprotonated molecules, four H-bonds are observed in each case as shown in Fig. 12(b) and (c), respectively. In addition to the two expected H-bonds, one H-bond of length 1.795 Å is formed between the glucose ring O atom and the C(7) hydroxyl H atom and another of length 1.860 Å is formed between the glucose-C(2) hydroxyl H atom and the O atom of the C(5)–OH group. Thus the bonding between the glucose and luteolin moieties is tridentate in Fig. 12(b) and (c). The B-ring twist angles for protonated and deprotonated luteolin-6-C-glucoside indicate A-, C-, B-ring coplanarity.

The product ion mass spectra of protonated (Fig. 8) and deprotonated (Fig. 6) luteolin-6-C-glucoside are dominated by product ions resulting from glycan cross-ring cleavages; such cleavages for the deprotonated molecule could be anticipated due to the tridentate bonding shown in Fig. 12(c). However, as shown in Fig. 12(a), there is but a single H-bond between the glucose and luteolin moieties. Yet the major cross-ring cleavages for protonated and deprotonated molecules are similar in that the ratio of $^{0,1}X^+$:$^{0,2}X^+$ intensities varies only by a factor

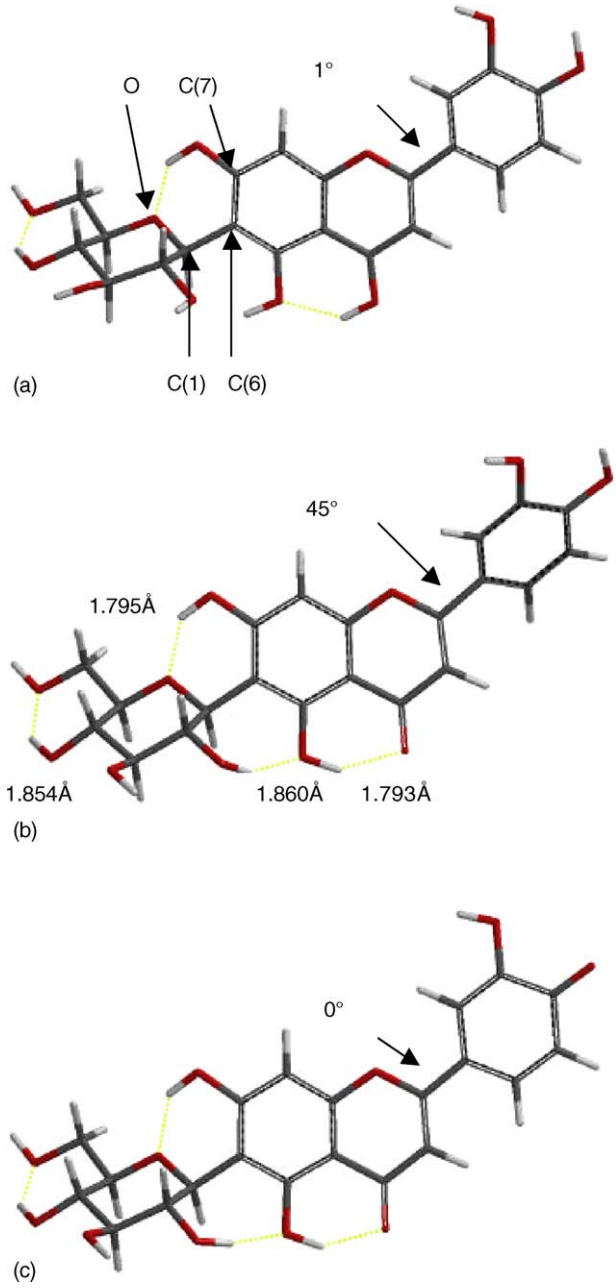

Fig. 12. Computed structures of luteolin-6-C-glucoside: (a) protonated; (b) neutral; (c) deprotonated. The arrow indicates the dihedral angle for B-ring twist.

of ∼4 from that of the $^{0,1}X^-$:$^{0,2}X^-$ ion intensities. Thus, perhaps there is a weak H-bond between the O atom of the C(2) hydroxy group in glucose and the H atom of the C(5)–OH group (Fig. 12(a)).

The computed structures for protonated, neutral, and deprotonated luteolin-8-C-glucoside (orientin) are basically similar to those for the 3′- and 4′-O-glucosides because the glucose-luteolin C–C bond is vicinal to but a single hydroxy group. Three H-bonds are observed for each structure. The B-ring twist angles for protonated, neutral and deprotonated luteolin-8-C-glucoside are −7, 45, and −1°, respectively. Again, due to the H-bond between the glucose and luteolin moieties, product ion mass spectra of protonated (Fig. 5(b)) and deprotonated (Fig. 4(b)) luteolin-8-C-glucoside are dominated by ions resulting from glycan cross-ring cleavages.

In summary, the computed structures for the 7-O, 6-C, and 8-C glucosides of luteolin can be interpreted so as to yield product ion mass spectra that are in good agreement with observations. However, the computed structures for protonated and deprotonated luteolin-4′-O-glucoside show an additional H-bond between the glycan and luteolin moieties that appears to be entirely ineffective in directing fragmentation.

5. Conclusions

From the examination of product ion mass spectra obtained at a collision energy of 46–47 eV, 3-O-, 7-O-, and 4′-O-glycosidic flavonoids have been differentiated, as have 6-C- and 8-C-glycosidic flavonoids; in addition, a method for differentiating between glucosides and galactosides has been proposed. It has been possible to identify criteria, shown in Table 6, for the discrimination of all of the isomers examined. The criteria have been identified from the wide variety of fragmentation processes due to cleavage of the glycon to produce both radical and even-electron flavone ions, and both C-ring and glycan cleavages observed in the product ion mass spectra of protonated and deprotonated flavonoid glycosides.

A particularly interesting criterion is the observation of the product ion of *m*/*z* 145 from protonated quercitin-3-O-galactoside. The elemental composition of *m*/*z* 145 was determined by accurate mass measurement as $C_6H_9O_4^+$; this product ion is unique to protonated quercitin-3-O-galactoside and is identified as the B^+–H_2O ion. The product ions of *m*/*z* 271 and 272 from protonated orientin are the first observed examples of ions that have been formed by neutral losses of part of the glycan and part of the flavonoid.

Chemical computations of the structures of the precursor ions indicate extensive intramolecular hydrogen bonding together with rotation of the B-ring to form coplanar flavonoid structures. The joint effects of hydrogen bonding and B-ring rotation that allows for resonance whereby the B and C rings develop an ethylenic bridge appear to play a major role in determining the fragmentation pathways of lowest activation energy. The computed structures of deprotonated homoorientin with proton loss from the 4′-hydroxyl group show that the combined effect of the C-glycosidic bonding, two strong H-bonds, and the ethylenic linkage between the C and B rings due to resonance is to shrink the ion and to bring about A-, C-, and B-ring coplanarity. There is a loss of entropy in what may be an example of cooperative interactive bonding; such positive cooperativity arises when the dynamic motion of a central chain is reduced by the formation of H-bonds.

Acknowledgements

The authors acknowledge the financial support from each of the Natural Sciences and Engineering Research Council of Canada (Discovery Grants Program), the Canada Foundation for Innovation, the Ontario Research & Development Challenge Fund, and Trent University.

References

[1] B.A. Bohm, Introduction to the Flavonoids, Harwood Academic, 1998.
[2] J.B. Harborne (ed.), The Flavonoids: Advances in Research since 1986, Chapman and Hall, London, 1994.
[3] E. Sjostrom, Wood Chemistry Fundamentals and Applications, Academic Press Inc., New York and London, 1981.
[4] E.C. Bate-Smith, in: W.E. Hillis (Ed.), Wood Extractives and Their Significance to the Pulp and Paper Industries, Academic Press Inc., New York and London, 1962, p. 133.
[5] R.A. Dixon, D. Ferreira, Phytochemistry 60 (2002) 205.
[6] J.B. Harborne, R.J. Grayer, in: J.B. Harborne (Ed.), The Flavonoids: Advances in Research since 1986, Chapman and Hall, London, 1994, p. 589.
[7] V. Beck, E. Unterrieder, L. Krenn, W. Kubelka, A. Jungbauer, J. Ster. Biochem. Mol. Biol. 84 (2003) 259.
[8] S.M. Boue, T.E. Wiese, S. Nehls, M.E. Burow, S. Elliott, C.H. Carter-Wientjes, B.Y. Shih, J.A. McLachlan, T.E. Cleveland, J. Agric. Food Chem. 51 (2003) 2193.
[9] B.W. Shirley, Trends Plant Sci. 1 (1996) 377.
[10] K.L. Fritz, C.M. Seppanen, M.S. Kurzer, A.S. Csallany, Nutrit. Res. 23 (2003) 479.
[11] R.A. Dixon, C.L. Steel, Trends Plant Sci. 4 (1999) 394.
[12] C. Gerhauser, K. Klimo, E. Heiss, I. Neumann, A. Gamal-Eldeen, J. Knauft, G.Y. Liu, S. Sitthimonchai, N. Frank, Mutation Res. 523 (2003) 163.
[13] B.M. Collins, J.A. McLachlan, S.F. Arnold, Steroids 62 (1997) 365.
[14] A.-C. Hopert, A. Beyer, K. Frank, E. Strunck, W. Wunsche, G. Vollmer, Environ. Health Perspect. 106 (1998) 581.
[15] R. Miksicek, J. Mol. Pharm. 44 (1993) 37.
[16] J.D.J. Kellis, L.E. Vickery, Science 225 (1984) 1032.
[17] L. Packer, G. Rimach, F. Virgili, Free Radic. Biol. Med. 27 (1999) 704.
[18] A. Sakushima, S. Nishibe, Phytochemistry 27 (1988) 915.
[19] F. Cuyckens, M. Claeys, J. Mass Spectrom. 39 (2004) 1;
F. Cuyckens, M. Claeys, J. Mass Spectrom. 39 (2004) 461 (Erratum).
[20] F.W. Crow, K.B. Tomer, J.H. Looker, M.L. Gross, Anal. Biochem. 155 (2) (1986) 286.
[21] A. Sakushima, S. Nishibe, T. Takeda, Y. Ogihara, Mass Spectrometry 36 (1988) 71.
[22] M. Becchi, D. Fraisse, Biomed. Environ. Mass Spectrom. 18 (2) (1989) 122.
[23] Q.M. Li, H. Van den Heuvel, L. Dillen, M. Claeys, Biol. Mass Spectrom. 21 (4) (1992) 213.
[24] Q.M. Li, M. Claeys, Biol. Mass Spectrom. 23 (7) (1994) 406.
[25] M. Takayama, T. Fukai, T. Nomura, K. Nojima, Rapid Commun. Mass Spectrom. 3 (1) (1989) 4.
[26] M. Takayama, T. Fukai, T. Nomura, K. Nojima, Shitsuryo Bunseki 37 (4) (1989) 239.
[27] M. Claeys, NATO ASI Ser., Ser. C 521 (Fundamentals and Applications of Gas Phase Ion Chemistry) (1999) 165.
[28] C. Borges, P. Martinho, A. Martins, A.P. Rauter, M.A. Almoster Ferreira, Rapid Commun. Mass Spectrom 15 (2001) 1760.
[29] S.H. Hansen, A.G. Jensen, C. Cornett, I. Bjørnsdottir, S. Taylor, B. Wright, I.D. Wilson, Anal. Chem. 71 (1999) 5235.
[30] A. Lommen, M. Godejohann, D.P. Venema, P.C.H. Hollman, M. Spraul, Anal. Chem. 72 (2000) 1793.
[31] I. Wawer, A. Zielinska, Mag. Res. Chem. 39 (2001) 374.
[32] V. Švehlíková, R.N. Bennett, F.A. Mellon, P.W. Needs, S. Piacente, P.A. Kroom, Y. Bao, Phytochemistry 65 (2004) 2323.
[33] Y.Y. Lin, K.J. Ng, S. Yang, J. Chromatogr. 629 (2) (1993) 389.
[34] M.S. Lee, D.J. Hook, E.H. Kerns, K.J. Volk, I.E. Rosenberg, Biol. Mass Spectrom. 22 (1) (1993) 84.
[35] M. Saegesser, M. Meinzer, J. Am. Soc. Brew. Chem. 54 (3) (1996) 129.
[36] A. Raffaelli, G. Moneti, V. Mercati, E. Toja, J. Chromatogr. A 777 (1) (1997) 223.
[37] S. Chimichi, V. Mercati, G. Moneti, A. Raffaelli, E. Toja, Nat. Prod. Lett. 11 (3) (1998) 225.
[38] J.F. Stevens, A.W. Taylor, M.L. Deinzer, J. Chromatogr. A 832 (1–2) (1999) 97.
[39] B. Ameer, R.A. Weintraub, J.V. Johnson, R.A. Yost, R.L. Rouseff, Clin. Pharmacol. Ther. (St. Louis) 60 (1) (1996) 34.
[40] J.F. Stevens, E. Wollenweber, M. Ivancic, V.L. Hsu, S. Sundberg, M.L. Deinzer, Phytochemistry 51 (6) (1999) 771.
[41] B. Boss, E. Richling, P. Schreier, Nat. Prod. Anal., [Symp.] P. Schreier (ed.), (1998). Meeting Date 1997, p. 187.
[42] T.R. Croley, R.J. Hughes, C.D. Metcalfe, R.E. March, Rapid Commun. Mass Spectrom. 14 (16) (2000) 1494.
[43] T.R. Croley, R.J. Hughes, C. Hao, C.D. Metcalfe, R.E. March, Rapid Commun. Mass Spectrom. 14 (23) (2000) 2154.
[44] R.J. Hughes, T.R. Croley, C.D. Metcalfe, R.E. March, Int. J. Mass Spectrom. 210–211 (2001) 371.
[45] N. Fabre, I. Rustan, E. de Hoffmann, J. Quetin-Leclercq, J. Am. Soc. Mass Spectrom. 12 (2001) 707.
[46] F. Cuyckens, R. Rozenberg, E. de Hoffmann, M. Claeys, J. Mass Spectrom. 36 (2001) 1203.
[47] Y.-L. Ma, F. Cuyckens, H. Van den Heuvel, M. Claeys, Phytochem. Anal. 12 (2001) 159.
[48] R.E. March, X. Miao, Int. J. Mass Spectrom. 231 (2004) 157.
[49] R.E. March, X.-S. Miao, C.D. Metcalfe, M. Stobiecki, L. Marczak, Int. J. Mass Spectrom. 232 (2004) 171.
[50] M. McCullagh, C.A.M. Periera, J.H. Yariwake, High throughput characterization of C-glycosidic flavonoids from Brazilian *Passiflora* species using LC-MS exact mass measurement and in-source CID, 19th Montreux Symposium, Montreux, Switzerland, 6–8 November, 2002.
[51] E. Hvattum, Rapid Commun. Mass Spectrom. 16 (2002) 655.
[52] E. Hvattum, D.J. Ekeberg, J. Mass Spectrom. 38 (2003) 43.
[53] M. Pikulski, J.S. Brodbelt, J. Am. Soc. Mass Spectrom. 14 (2003) 1437.
[54] X.-S. Miao, C.D. Metcalfe, R.E. March, in: Proceedings of the 53rd ASMS Conference on Mass Spectrometry and Allied Topics, San Antonio, TX, 2005, CD.
[55] J. Zhang, J.S. Brodbelt, J. Am. Chem. Soc. 126 (2004) 5906.
[56] J. Zhang, J.S. Brodbelt, Analyst 129 (2004) 1227.
[57] T. Iwashina, J. Plant Res. 113 (2000) 287.
[58] K.R. Markham, Techniques of Flavonoid Identification, Academic Press, London, 1982.
[59] E. Lewars, Computational Chemistry, Kluwer, Boston, 2004 (Chapter 6).
[60] Wavefunction Inc., 18401 Von Karman Avenue, Suite 370, Irvine, CA 92612.
[61] M.J.S. Dewar, E.G. Zoebisch, E.F. Healy, J.J.P. Stewart, J. Am. Chem. Soc. 107 (1985) 3902.
[62] J.J.P. Stewart, J. Comp. Chem. 10 (1989) 209, 221;
J.J.P. Stewart, in: P.v.R. Schleyer, N.L. Allinger, T. Clark, J. Gasteiger, P.A. Kollman, H.F. Schaefer III, P.R. Schreiner (Eds.), PM3, Encyclopedia of Computational Chemistry, vol. 3, Wiley, Chichester, 1998, p. 2080.
[63] E. Lewars, Computational Chemistry, Kluwer, Boston, 2004 (Chapter 2).
[64] Y.L. Ma, Q.M. Li, H. Van den Heuvel, M. Claeys, Rapid Commun. Mass Spectrom. 11 (1997) 1357.
[65] B. Domon, C. Costello, Glycoconjugate J. 5 (1988) 397.
[66] R.E. March, C.J. Stadey, Rapid Commun. Mass Spectrom. 19 (2005) 805.
[67] D.H. Williams, E. Stephens, M. Zhou, J. Mol. Biol. 329 (2003) 389.
[68] P. Gilli, V. Ferretti, G. Gilli, P.A. Borea, J. Phys. Chem. 98 (1994) 1515.